ChemPubSoc Europe

DOI: 10.1002/open.201900339

Open Access ChemistryOPEN Reviews

Special Collection

Molecular and Supramolecular Multiredox Systems

Jyoti Shukla, Vijay Pal Singh, and Pritam Mukhopadhyay*[a]

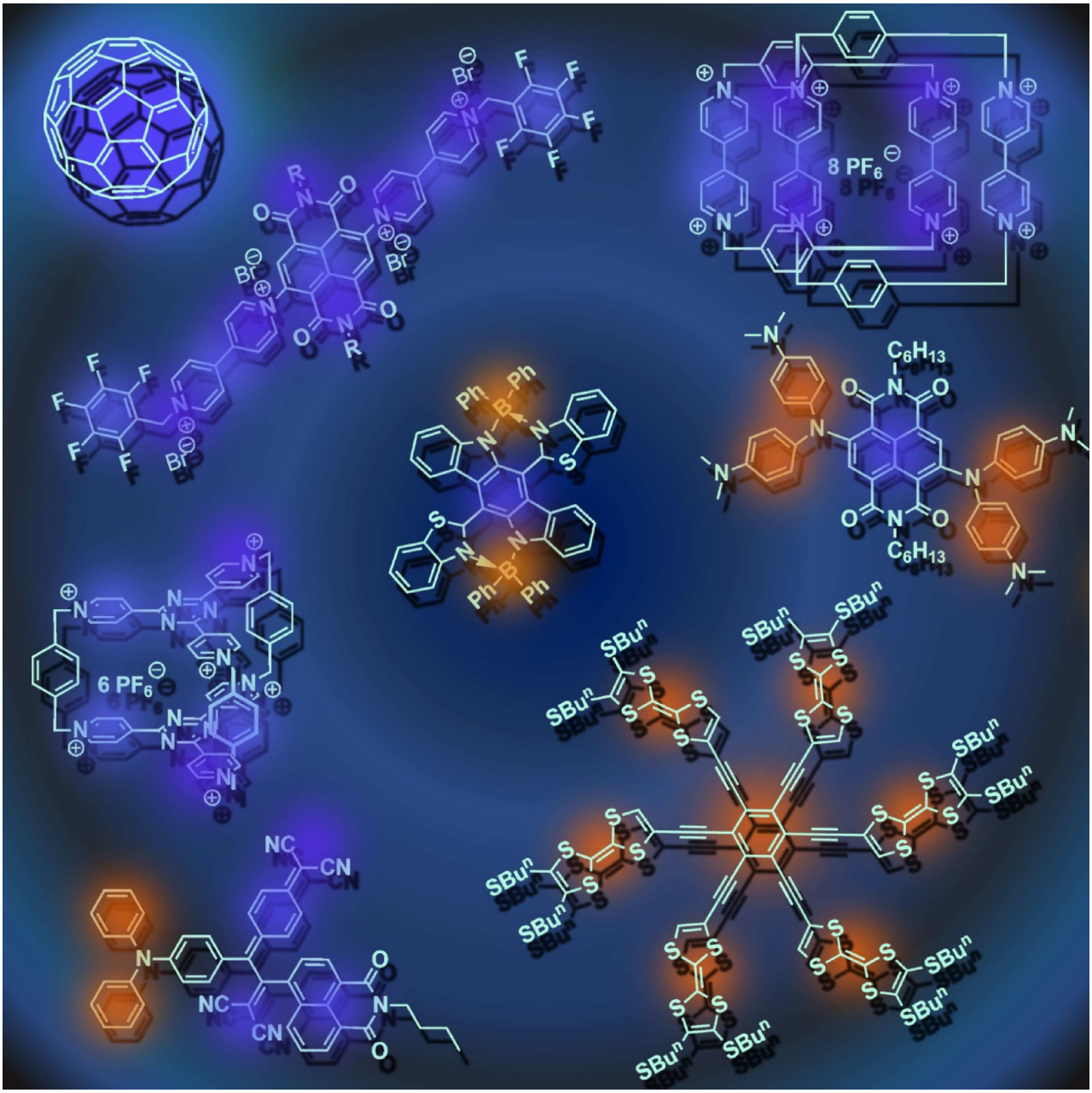

The design and synthesis of molecular and supramolecular multiredox systems have been summarized. These systems are of great importance as they can be employed in the next generation of materials for energy storage, energy transport, and solar fuel production. Nature provides guiding pathways and insights to judiciously incorporate and tune the various molecular and supramolecular design aspects that result in the formation of complex and efficient systems. In this review, we have classified molecular multiredox systems into organic and organic-inorganic hybrid systems. The organic multiredox systems are further classified into multielectron acceptors, multielectron donors and ambipolar molecules. Synthetic chemists have integrated different electron donating and electron withdrawing groups to realize these complex molecular systems. Further, we have reviewed supramolecular multiredox systems, redox-active host-guest recognition, including mechanically interlocked systems. Finally, the review provides a discussion on the diverse applications, e.g. in artificial photosynthesis, water splitting, dynamic random access memory, etc. that can be realized from these artificial molecular or supramolecular multiredox systems.

1. Introduction

Multiredox systems have major importance in wide ranging areas such as high energy density batteries, solar fuel production, catalysis, sensors, photosynthesis, and cellular respiration. Research progress in synthetic and supramolecular chemistry has led to complex artificial systems that can attempt to mimic intricate biological processes.[1] Countless biological processes require multielectron transfer reactions for conversion of energy that can be utilized for chemical transformations.[2] These processes involve proton and electron tunneling, light absorption, excited electronic state formation and excited state energy transfer. These processes occur in cellular respiration, photosynthesis, DNA UV-damage repairs, neurotransmitters and many other complex biological reactions.[3] Multiple electron transfer reactions can also have great importance in those biological processes which require stable reduced and oxidized intermediate states of organic molecules.[4]

Most of the practically important electrochemical reactions such as photosynthesis, proton reduction, CO_2 splitting and water oxidation are multi-electronic in nature and have substantial kinetic barriers for electron transfer.[5,6] Therefore, for the practical sense of required energy input, we need to design the electrode surface in such a way that can increase the electron transfer rate. Thermodynamically simple processes like, hydrogen oxidation and dioxygen reduction also have multi-electronic nature and requires multiredox active electrocatalysts to accelerate the reaction rate. Nature gives us valuable lessons about how to assemble such complex self-assemblies with precisely defined functional components.[7]

There is a significant challenge for material and biological scientists to design and synthesize such complex molecular materials which can store and transfer multiple electrons at low operational potentials to the substrate and are stable under ambient condition.[7c] In this review article, we make an effort to provide a concise overview of the recent multiredox systems.

2. Classification of Multiredox Systems

A large class of molecular and supramolecular redox systems have been synthesized having attractive optical and electronic properties. The multiredox systems of interest, in this review, are that can perform at least four-electron transfer processes. We have classified multiredox systems in three broad categories:

1. Organic multiredox molecules
2. Organic-Inorganic Hybrid multiredox molecules
3. Supramolecular multiredox systems

2.1. Organic Multiredox Molecules

Construction of multiredox active organic molecules are of particular interest owing to their importance in advanced functional materials and also as molecular catalysts for multi-electron transformation processes.[8] These multiredox active organic scaffolds can vary from small molecules, dendrimers to oligomers and polymers.[9] Depending on their electronic properties, these multiredox active molecues can be further categorized into three classes: I. Multielectron acceptors, II. Multielectron donors, and III. Multielectron ambipolar systems, which can donate and accept the multiple electrons simultaneously.

2.2. 1. Organic Multi-electron Acceptors

For the past three decades, synthesis of organic molecules with strong electron accepting and n-type semiconducting properties have been stimulated by the global need for efficient and cheap electronic devices to access renewable energy sources.[10] Towards this endeavour, an understanding of the elementary relationship between the molecular and supramolecular structures and their opto-electronic properties are needed. In general, the multielectron acceptors are constructed by con-

[a] Dr. J. Shukla, V. P. Singh, Prof. Dr. P. Mukhopadhyay
Supramolecular and Material Chemistry Lab
School of Physical Sciences
Jawaharlal Nehru University
New Delhi-110067 India
E-mail: m_pritam@mail.jnu.ac.in

Special Collection An invited contribution to a Special Collection dedicated to Functional Supramolecular Systems

jugating electron deficient functional groups or electronegative atoms with a π-scaffold.[11] The electronic coupling between the functional groups enhance the overall electron deficiency of the molecular system.

Fullerene (C_{60}) **OA1** was demonstrated as one of the first multistate redox active molecule, which could act as a multi-electron acceptor. Cyclic voltammetry (CV) and Differential Pulse Voltammetry (DPV) studies at −10 °C displayed six well-separated reduction waves (five reversible and one pseudo-reversible).[12] Excellent electron accepting ability, favorable LUMO energy level and facile reversible reduction of fullerene and its derivatives has facilitated its application in bulk heterojunction organic photovoltaics, ferromagnetic charge-transfer salts, and alkali metal intercalated superconducting complexes.[13]

Recently, Benniston and co-workers have reported a disulfide-strapped viologen derivative **OA2** (Scheme 1).[14] The CV studies of **OA2** shows reduction waves with $E_{1/2}$ at −0.03 V, −0.16 V, −1.26 V and −1.54 V versus Ag/AgCl. Lichtenberger and co-workers studied the reduction of a similar molecule having methyl viologen groups (**OA3**) and its theoretical simulation studies.[15] It was found that the first electron reduces the bipyridinium moiety while the second reduction of the one-electron reduced bipyridinium moiety results in the fast intra-molecular two-electron transfer towards the reductive cleavage of the disulfide moiety to form dithiolate. After the intra-molecular electron transfer and S–S bond cleavage the bipyridinium molecule undergoes two single electron reductions at more negative potentials. Hence, this multiredox active bipyridinium molecule provides a low energy pathway for the reductive cleavage of the disulfide bond, as cleavage of S − S bond is an important reaction for many biological and chemical processes.

Conjugated viologen scaffolds can be intelligently applied to design novel eight-electron acceptors. Along this line, the Stoddart group reported the synthesis of an octa-cationic tetraviologen-based rigid cyclophane **OA4** (Scheme 1).[16] This molecule possesses a highly electron deficient rectangular cage, which can accept up to eight electrons and encapsulates two small-sized aromatic guests simultaneously or one large-sized guest molecule. The CV analysis of **OA4** shows the first reduction peak with $E_{1/2}$ at −0.17 V vs Ag/AgCl for the four-electron transfer process, which reduces all the four bipyridinium moieties to yield tetraradical tetra-cationic system. Simultaneous four-electron reduction indicates that there is no electronic communication between the four bipyridinium moieties in spite of the *p*-phenylene bridge. The next two reduction waves at −0.48 V and −0.62 V vs Ag/AgCl, each for the two-electron transfer process indicates the presence of electronic communication between the two comparably planar bipyridinium radical cation through the *p*-phenylene bridge.

The Stoddart group has further reported the synthesis and electrochemical studies of macrobicyclic cyclophane consisting of two electron-poor triazines scaffolds conjugated with six pyridinium rings and *p*-xylyl units as the bridging units (**OA5**, Scheme 1).[17] These positively charged moieties endow the cyclophane with outstanding electron deficiency, which turns the cage into a strong receptor for electron-rich aromatic hydrocarbons. The CV of this molecule shows the eight-electron accepting the property with six electrochemically accessible redox states. The first three reductions at −0.29 V, −0.65 V and −1.07 V for the six pyridinium moieties are related to two-electron transfer processes indicating the absence of electronic

Jyoti Shukla received her B. Sc. and and M. Sc. degrees from Chhatrapati Shahu Ji Maharaj University Kanpur, India. She did her Ph.D. under the supervision of Dr. Pritam Mukhopadhyay at Jawaharlal Nehru University, New Delhi. Her research interests are in the areas of modulation of band gap in organic dyes for solar cell application, synthesis of stable zwitterionic radicals as ground state electron donors, multistate electron reservoir systems for their application in advanced energy storage systems. She is also involved in the studies of counter anion dependent organic proton conducting materials for application in fuel cell, synthesis of molecular boxes with supramolecular and material properties.

Vijay Pal Singh received his B.Sc. and and M.Sc. degrees from Mahatma Jyotiba Phule Rohilkhand University Bareilly, India. To pursue his Ph.D. he joined Dr Pritam Mukhopadhyay's group at Jawaharlal Nehru University, New Delhi in 2016. His research interests are: design and synthesis of naphthalenediimide macrocycles, corona-arene-based pillar [n]-quinones and Rotaxanes.

Pritam Mukhopadhyay obtained his Ph.D. from IIT Kanpur, India under the guidance of Prof. P. K. Bharadwaj. He then joined the group of Prof. L. Isaacs at the University of Maryland, College Park, USA as a post-doctoral fellow, where he worked on the synthesis and studies of complex self-sorting systems. Later, he worked in the area of supramolecular gels as a JSPS fellow with Prof. S. Shinkai at the Kyushu University, Japan. He then joined the School of Physical Sciences, Jawaharlal Nehru University, New Delhi, India, where he is currently an Associate Professor. His group's research interest involves synthesis and stabilization of organic radical ions, highly electron-deficient and electron-rich systems and applications related to electron transfer reactions. The group is also interested in the design and synthesis of supramolecular materials, e.g. ferroelectric, piezoelectric, NLO-active and magnetic materials. The other interest of the group has been in the synthesis of hybrid antimalarials and redox-active anticancer agents.

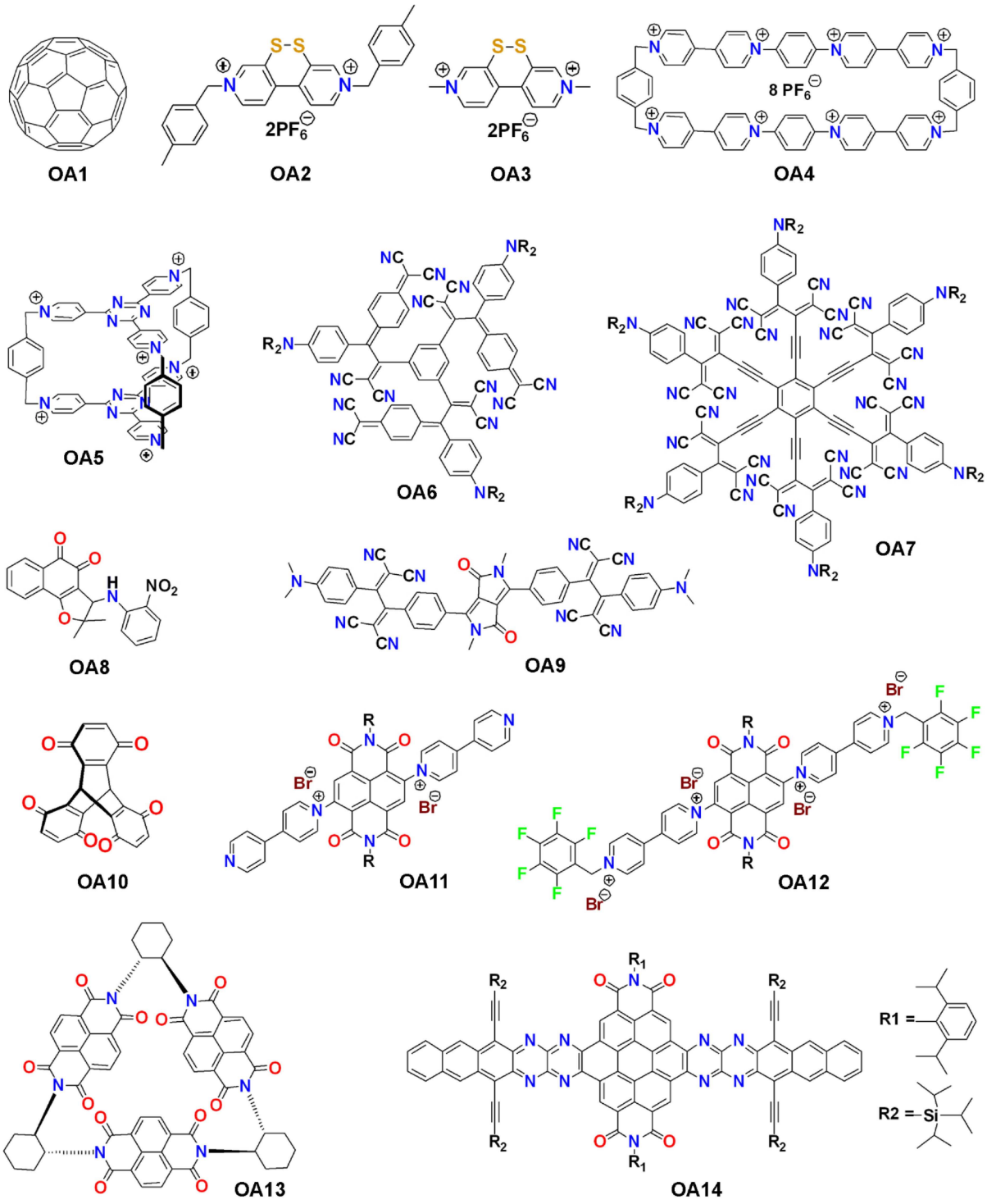

Scheme 1. Molecular structures of various organic multielectron acceptor molecules.

communication between the two triazine platforms. The last two separate reduction waves at −1.44 V and −1.66 V for triazine moieties indicate the restoration of electronic communication between the two triazine platforms after six-electron reduction.

In a pioneering development, Diederich and co-workers prepared multielectron acceptor **OA6** by the regioselective [2+2] cycloaddition reaction between N,N-dialkylanilino-substituted alkynes and 7,7,8,8-tetracyanoquinodimethane, followed by ring opening of the primarily formed cyclobutenes (Scheme 1).[18] The electrochemical analysis of **OA6** revealed six reversible reduction waves at −0.50 V, −0.64 V, −0.76 V, −0.84 V, −0.98 V, −1.14 V vs Fc^{+}/Fc, which confirms the strong electronic communication between all the moieties. This group

also reported multivalent dendrimer-type charge transfer chromophore **OA7** by the thermal [2+2] cycloaddition reaction between tetracyanoethylene and corresponding electron rich alkyne.[19] **OA7** is capable of taking up electrons at +0.89, −0.46, −0.60, −0.70, −0.76, −0.95, −1.07 and −1.57 V vs Fc+/Fc, therefore representing its molecular battery like property.

The synthesis and biological activities of multiredox active nor-β-lapachone derivatives **OA8** (Scheme 1) having quinone and the nitroaromatic groups have been reported. These compounds show the cytotoxic activity against tumor cell lines and also work as trypanocidal agents.[20] For explaining the biological activities of nor-β-lapachone derivatives, Frontana and co-workers have studied the various redox states of this molecule by experimental and theoretical studies.[21] The CV of this compound shows the four single electron reduction waves with the $E_{1/2}$ value of −1.20 V, −1.61 V, −1.73 V and −2.45 V vs Fc/Fc^+ with first three being reversible and the last cathodic wave being irreversible. The first electron reduces the quinone moiety to form the quinone radical anion, while the second electron reduction involves the formation of biradical dianion state, in which both unpaired electrons are located on the quinone and the nitro group. The third electron is accumulated by the electrogenerated radical anion of the quinone scaffold to form the corresponding dianion. On the basis of the potential relationship with experimental selectivity, they suggested that the anticancer activities of these compounds are related to the formation of stable dianion biradical species while the trypanocidal activity depends on the formation of stable semiquinone intermediate.

Kanbara's group synthesized donor-acceptor conjugated dioxopyrrolopyrrole (DPP) derivative with electron-withdrawing 1,1,4,4-tetracynobutadiene (TCBD) groups and electron-donating NMe_2 phenyl groups **OA9** (Scheme 1).[22] This molecule can accept up to five electrons. The CV results show three reversible reduction waves at −0.88 V, −1.20 V and −1.98 V with the first two waves being for the two-electron transfer, while the last one is for one-electron process. The first and second peak are assigned to the reduction of two TCBD groups. The presence of two two-electron reduction waves indicates that there is no electrochemical interaction between the two TCBD moieties through the DPP core. The last cathodically shifted wave is assigned to the reduction of DPP moiety and the relatively large negative potential for the DPP reduction is explained by the electron donating effect of the dianionic TCBD groups.

In another effort to design new multielectron acceptors, Park and co-workers reported a compact tripodal triptycene-based molecule bearing three quinone units **OA10** (Scheme 1).[23] The electrochemical analysis of **OA10** revealed distinct five one-electron reduction peaks in DPV. The first three reduction happens at −0.58 V, −0.77 V and −0.94 V vs Ag/AgCl due to the formation of benzoquinone radical anions, while the other two peaks at −1.44 V and −1.59 V vs Ag/AgCl are related to the second reduction of the benzoquinone units. These excellent redox properties deliver Li-ion coin cells with specific capacity of 387 $mA\,h\,g^{-1}$. This triptycene based electrode provide a specific energy of up to 1032 $W\,h\,kg^{-1}$ at the rate of 0.1 C.

In a recent report, we demonstrated bis-substitution of 4,4′-bipyridnium units at the naphthalenediimide-core (cNDI), which provides a multi-electron acceptor **OA11** with excellent yields of 85%.[24] CV results of **OA11** revealed four reversible reduction waves at 0.00 V, −0.40 V, −1.02 V and −1.15 V vs SCE with a low-lying LUMO of −4.43 eV. Further reaction of **OA11** with the differently substituted benzyl bromides resulted in the formation of tetra-cationic six-electron acceptors and also exhibited multiple anion-π interactions. For example, **OA12** shows the six reduction waves at +0.05 V, −0.18 V, −0.27 V, −0.58 V, −0.75 V and −1.00 V vs SCE with excellent reversibility. These new class of electron acceptors were termed as 'Electron-sponge' due to its ability to accumulate six-electrons at low potentials and within a remarkably narrow potential range.

Stoddart and co-workers synthesized a rigid redox-active NDI-based molecular prism (**OA13**, Scheme 1) in 25% yield.[25] The through-space orbital interaction and additional electron sharing phenomena was proved by experimental and theoretical calculations. The CV analysis revealed presence of six well-separated reduction waves from −0.56 V to −1.51 V vs Ag/AgCl. The molecular triangle has been applied in rechargeable lithium-ion batteries with capacity of 146.4 $mA\,h\,g^{-1}$ at low current rates.[26]

In another effort to have novel one-dimensionally long multi-electron acceptors, Bunz et al. reported the synthesis of large coronene-containing N-heteroarenes containing thirteen rings integrated in a row **OA14** (Scheme 1).[27] This coronene-azaacene based compound shows multielectron accepting properties as observed by the CV analysis, which revealed four reversible reductions waves at −0.35 V, −0.53 V, −0.86 V and −1.07 V vs Fc/Fc^+, with low-lying LUMO of −4.45 eV. Interestingly, highly red-shifted absorption in the Near Infrared (NIR) region was observed with λ_{onset} values reaching 1300 nm.

2.2.1. Organic Multi-electron Donor Molecules

Organic multielectron donors based on arylamines, aryloxy, tetrathiafulvalene (TTF), di-reduced NDI scaffolds have found applications in the field of multistate systems, polymer batteries, light-emitting devices, electrical conductivity, electroluminescence, electromagnetic and photorefractive materials. These molecules can be easily oxidized to its stable radical cationic states because of their low oxidation potential.[28]

[n]Radialenes (n = 4–6) having multiple 1,3-dithiole rings are known for their unique redox behaviour. Out of them [5] radialene with five 1,3-dithiol-2-ylidene units shows unique multiredox property as it can transfer four electrons simultaneously. Misaki and co-workers synthesized a TTF analog possessing two [5]radialene moieties **OD1** (Scheme 2).[29] DPV of molecule **OD1** shows a redox peak at −0.05 V vs Fc/Fc^+ in benzonitrile at room temperature for the simultaneous eight-electron transfer process. The single peak for eight-electron transfer process indicates the lack of electronic communication between the two [5]radialene moieties

Tanaka and his co-workers have synthesized pseudo-beltane-like cylindrical polymacrocyclic oligoarylamine (**OD2**,

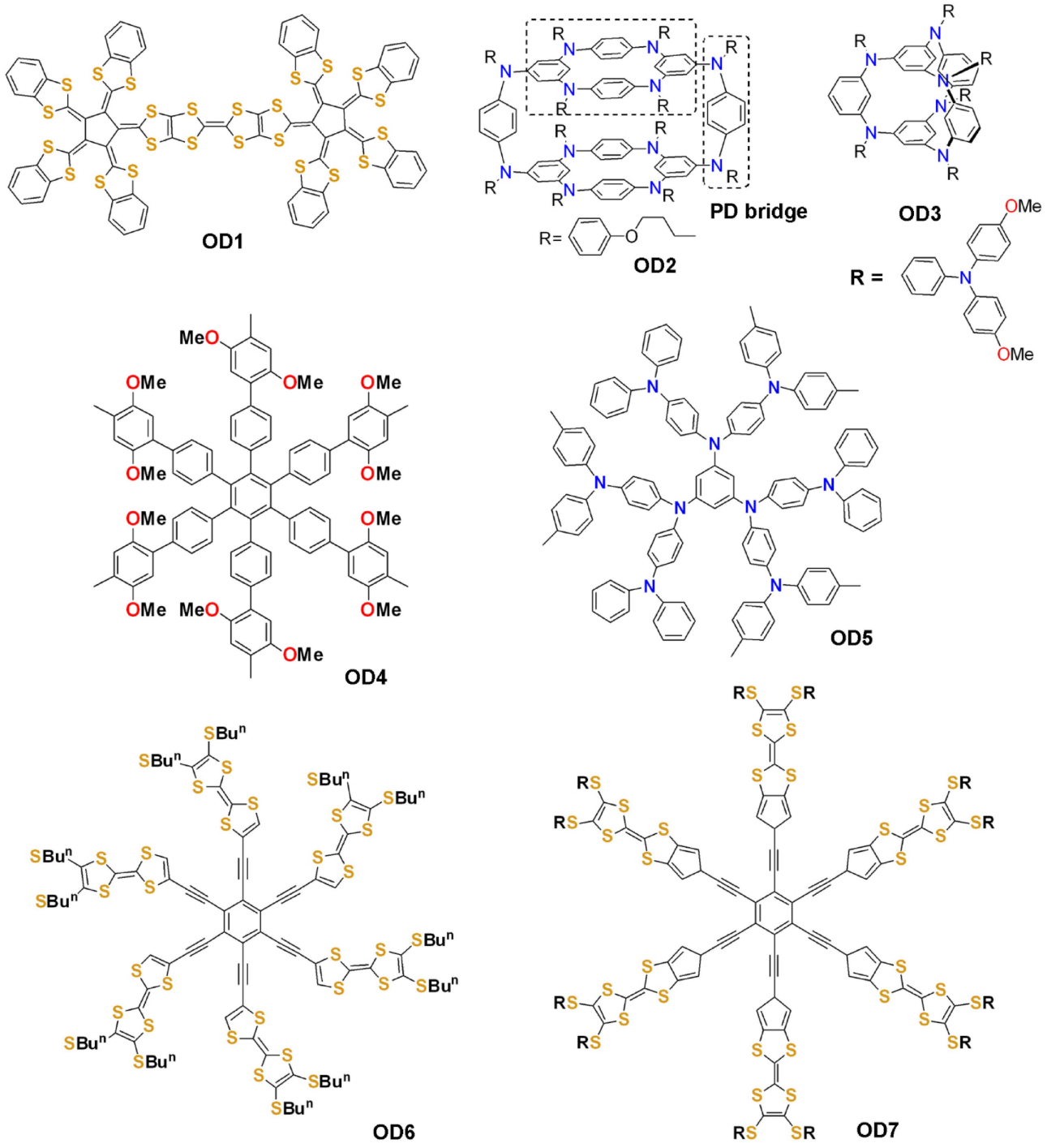

Scheme 2. Molecular structures of the multielectron donors.

Scheme 2).[30] This molecule can donate up to 12 electrons due to the presence of six *p*-phenylenediamine units. Six oxidation waves could be confirmed from CV/DPV studies: at −0.138 V (vs Fc/Fc+) for two-electron transfers, at +0.046 V and +0.137 V each for one-electron transfer, at +0.292 V for four-electron transfers, at +0.511 V for two-electron transfers and at +0.560 V, +0.598 V for each one-electron transfer processes. Therefore, **OD2** can be oxidized up to a dodeca-cationic state on the electrochemical time scale. The diradical di-cationic and tetraradical tetra-cationic species generated by chemical oxidation of compound **OD2** exhibits the high spin states at low temperature.

Ito and co-workers have reported the synthesis and analysis of double- and triple-decker 1,3,5-benzenetriamine-based compounds.[31] The N-dianisylaminophenyl group substituted double-decker **OD3** molecule shows unique multiredox activity (Scheme 2). This molecule can be oxidized up to dodeca-cationic state at the electrochemical timescale. The DPV of **OD3**

shows two broad peaks with a shoulder at the first peak. The simulation of DPV results of first peak suggests that the oxidation waves at −0.12 V (1e$^-$) vs Fc/Fc$^+$ and −0.06 V (1e$^-$) corresponds to the generation of dicationic state and at +0.03 V (4e$^-$) corresponds to the hexacationic state, while the simulation of the second peak suggests the dodeca-cationic state, which is formed by six-electron transfers at +0.44 V (1 e$^-$), +0.49 V (1 e$^-$), +0.51 V (1 e$^-$), +0.56 V (1 e$^-$), +0.60 V (1 e$^-$) and +0.61 V (1 e$^-$). Additionally, the polycationic species of **OD3** generated by the chemical oxidation with two and six equivalents of the oxidizing agent (tris(4-bromophenyl)aminium hexachloroantimonate) were found to be in the high spin state.

Along with the TTF and arylamines, arylmethoxy groups have also been applied to realize multielectron donors. Along this line, Rathore and co-workers synthesized multielectron donor **OD4** (Scheme 2) utilizing hexaphenylbenzene as a platform with six redox active 2,5-dimethoxytolyl groups.[32] In the CV analysis, this electron donor compound shows single oxidation wave at +1.15 V vs SCE for a simultaneous six-electron transfer process. Additionally, the chemical oxidation of **OD4** with $SbCl_5$ as the oxidizing agent generates the hexacationic-hexaradical species and can be isolated in the pure form. The generated multiply charged cationic-radical salt proved its application as an "*electron-sponge*" towards variety of electron donor molecules.

In 1998, Shirota and co-workers synthesized and analyzed an organic hyperbranched π-donor dendritic molecule of G1 generation consisting of tertiary aromatic amines (**OD5**, Scheme 2).[33] This dendritic molecule shows unique multiredox properties involving as many as nine-electron reversible oxidations. The CV of **OD5** exhibit six redox waves at 0.13 V, 0.30 V, 0.38 V, 0.56 V, 1.05 V and 1.22 V vs Ag/Ag$^+$. By coulometry analysis, they confirmed that the starting three waves are for one-electron transfer process and the fourth wave is for three-electron transfer process, while the last two waves are for one- and two-electron transfer processes, respectively.

Iyoda and co-workers reported TTF-hexamers with a flexible disk-like **OD6** and star-shaped **OD7**, which integrates the TTF groups with the benzene scaffold via alkyne linkers (Scheme 2).[34,35] These compounds displayed two six-electron oxidation waves with $E_{1/2}$ values of −0.13 V (**OD6**$^{6+}$), +0.05 V (**OD6**$^{12+}$) and 0.097 V (**OD7**$^{6+}$),0.37 V (**OD7**$^{12+}$) for **OD6** and **OD7** respectively. They also perfomed chemical oxidation of **OD6** and **OD7** using $Fe(ClO_4)_3$ as the oxidising agent. Furthermore, **OD6**$^{1+}$ radical cation self-assembled into hexagonal columnar fibrous material. The small tapes prepared from this self-assembled wire displayed conductivity of 1.1×10^{-3} S cm^{-1}.

2.2.2. Ambipolar Molecules

Multiredox active electrochemically ambipolar molecules, which can be accessed in both the oxidized and reduced states within an easily accessible potential window are important in both experimental and theoretical research.[36] The most common strategy to endow ambipolarity is to link multiredox active donor and acceptor (D–A) groups. This strategy needs the systematic choice of donor and acceptor units and introduction of particular electron donating and withdrawing substituents at the specific site to tune the HOMO and LUMO level to achieve the E_{ox} and E_{red} within a narrow electrochemical window.[37]

Recently, Mishra and his co-workers have reported the synthesis and photovoltaic application of D–A–A based multiredox active **OAm1** (Scheme 3).[38] In this molecule, the 1,8-naphthalimide as acceptor unit is conjugated with triphenylamine as the donor unit through dicyanoquino-dimethane as another acceptor unit. The CV results show the three multi-step reduction waves at −0.10 V, −0.29 V and −1.10 V vs SCE with an oxidation wave at +1.30 V corresponding to the oxidation of arylamine moiety. The organic photovoltaic cell based on compound **OAm1** showed excellent photon to current efficiency value of 6.11 %.

Radiaannulenes are cyclic molecules, which have endo and exocyclic double bonds and consequently lie between radialenes and annulenes. Nielsen and co-workers synthesized TTF coupled radiaannulene derivative (**OAm2**, Scheme 3).[39] This molecule shows the electrochemically accessible six-redox states with two reduced states, one neutral state and three oxidized states (−2/−1/0/+1/+2/+4). The CV results demonstrated three oxidation waves and two reduction waves. The first oxidation wave has small splitting with $E_{1/2}$ values of +0.20 V and +0.29 V vs Fc/Fc$^+$, which indicates oxidation of two TTF moieties to its radical cationic form. The third oxidation wave at +0.61 V is for the two-electron transfer processes. Additionally, **OAm2** shows two reduction peaks at $E_{1/2}$ value −1.16 V and −1.52 V corresponding to the formation of the radical anion and dianion species, respectively.

Bryce and co-workers reported the synthesis of multiredox active ambipolar molecules with extremely low band gap. They covalently linked TTF units with electron accepting TCNQ[40] **OAm3** or polynitrofluorene unit[41] **OAm4** (Scheme 3). Due to the presence of isolated linker (sigma bond) between two redox moieties, there is the negligible electronic interaction between the electron donor and acceptor scaffolds. The TTF-TCNQ diad **OAm3** revealed five electrochemical redox states with two oxidized and two reduced states, each having its distinct color. The oxidation occurs at −0.11 V and +0.43 V, while reduction at −0.24 V and −0.72 V (Fc/Fc$^+$), which results in one of the lowest band gap of 0.17 eV. Compound **OAm4** shows five reversible redox waves in CV analysis, for the stepwise two-electron oxidation at −0.10 V, −0.32 V and three-electron stepwise reduction at −0.38 V, −0.90 V and −1.56 V vs (Fc/Fc$^+$) with an extremely low band gap of 0.3 eV.

Fang et al. designed and synthesized a cruciform ladder-type molecule **OAm5**, which integrated a B←N coordination unit in a compact structure.[42] Molecule **OAm5** displayed well-separated two one electron reduction waves at −0.83 V, −1.14 V and two one- electron oxidation waves at +0.79 V, +1.30 V vs Ag/AgCl. Therefore, five distinct redox states were observed including the boron-containing radical ion. They also characterized each redox state by spectrochemical measurements and demonstrated the multicolour electrochromism with outstanding recyclability. Single crystal analysis of **OAm5** neutral state, reduced dinion and oxidized radical cation

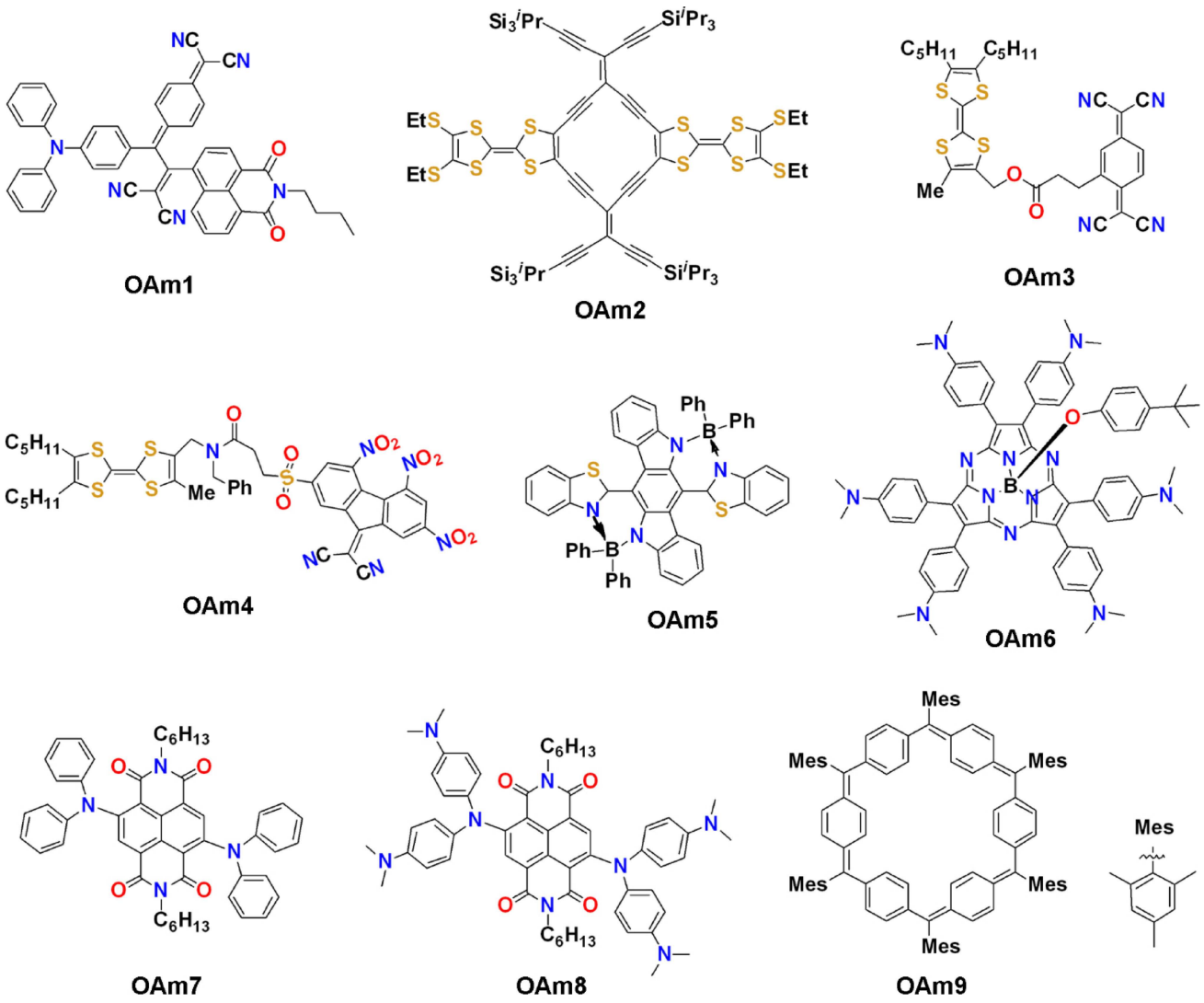

Scheme 3. Molecular structures of ambipolar compounds, showing multielectron donor and acceptor behaviour simultaneously.

revealed structural transformations into two different quinonoid structures during redox processes. They concluded that the B←N coordination play an important role in the robust multi-redox properties by modifying the π-electron density and extending the spin and charge delocalization.

Torres and co-workers have reported the peripherally hexa-arylated subporphyrazine molecules and demonstrated its ambipolar multiredox activity. Subporphyrazines are the aromatic compounds constructed by three pyrrole subunits linked through their 2,5-positions by aza-bridge.[43] The NMe_2 derivative of arylated subporphyrazines (**OAm6**, Scheme 3) shows ambipolar multiredox activity as it accepts three-electrons as well as donates up to six-electrons due to the presence of six amine groups.[46] The CV data of **OAm6** revealed three pseudo-reversible reduction waves at −1.56 V, −1.99 V and −2.28 V vs Fc/Fc^+, each for one-electron reduction process, with additional two irreversible oxidation waves at +0.38 V and +0.90 V, each for the three-electron transfer processes.

Our group reported a series of axially fused PMDA/NTCDA-TTF (PMDA: Pyromellitic dianhydride NTCDA: Naphthalenetetracarboxylic dianhydride), electrochemically ambipolar molecules with multiredox properties.[44] The CV/DPV analysis of PMDA based molecule, fused with the two TTF moieties, revealed three oxidation waves with $E_{1/2}$ value of +0.83 V, +0.93 V, +1.48 V, and two reduction waves at −1.33 V, −1.66 V. Recently our group demonstrated the first Buchwald−Hartwig reaction at the naphthalenediimide-core (c-NDI), leading to the coupling of various secondary aromatic amines.[45] Importantly, compound **OAm7** (Scheme 3) having diphenylamine donors and **OAm8** having Bindschedler's green leuco base showed blue to blackish-green colour. Compound **OAm8** exhibited λ_{max} of 830 nm with λ_{onset} values up to 1070 nm. These compounds manifested multi-electron reservoir properties, with **OAm8** exhibiting a total of eight-redox states and a remarkably low band gap of 0.95 V.

Wu and co-workers reported a novel [6]cyclo-para-phenylmethine macrocycle (**OAm9**, Scheme 3).[46] The molecule was

found to be globally aromatic due to conjugation of 30 π-electrons. CV analysis revealed multi-redox behaviour with two reductions at −1.918 V and −2.048 V, and six oxidations +0.116 V, +0.534 V, +0.783 V, +0.880 V, +0.919 V, and +1.042 V (vs Fc+/Fc). The chemical oxidation of **OAm9** with SbF_6 provides radical cation, dication, and radical trication. The radical cation and the trication showed broad absorption in NIR region with λ_{max} at 1126 nm and 2021 nm, respectively. The dication showed antiaromatic, open shell di-radical character, and displayed an intense absorption band with λ_{max} at 807 nm with a weak tail up to 1500 nm.

2.3. Hybrid Multiredox Molecules

Multicomponent based hybrid redox materials continue to be a research area of current interest due to their diverse application in the field of functional molecular materials.[47] These systems are not only important for their molecular properties like magnetism and electrical conductivity, but they can also play an important role in the field of catalysis, host-guest interactions, and in electron reservoirs, etc. For the synthesis of these materials, the most crucial point is the choice of appropriate redox component.[48] For introducing the multi-redox activity in the multicomponent system, the inclusion of transition metals can be a promising tool as they exhibit variable oxidation states. Besides their redox properties, these materials also provide the route for self-assembled supramolecular arrays.[49]

Lehn and co-workers were the very early proponents of organic-inorganic hybrid multiredox systems. In this pioneering work, they reported a series of $[M_4^{II}L_4]^{8+}$ [2×2] grid type complexes with variable ligands and metal ions. All the metal complexes showed multiredox properties, out of which one example is presented here (**H1**, Scheme 4) with maximum numbers of reduction steps. The complex **H1** comprises of Co (II) as the central metal atom and amine ligands having two ester groups.[50] The CV analysis in DMF revealed twelve reversible, well-resolved, one-electron reduction waves at room temperature in DMF with redox potential ranging from −0.45 V to −2.20 V vs Fc/Fc^+ (−0.45 V, −0.50 V, −0.63 V, −0.75 V, −1.03 V, −1.24 V, −1.45 V, −1.62 V, −1.89 V, 2.05 V, −2.12 V and −2.20 V).

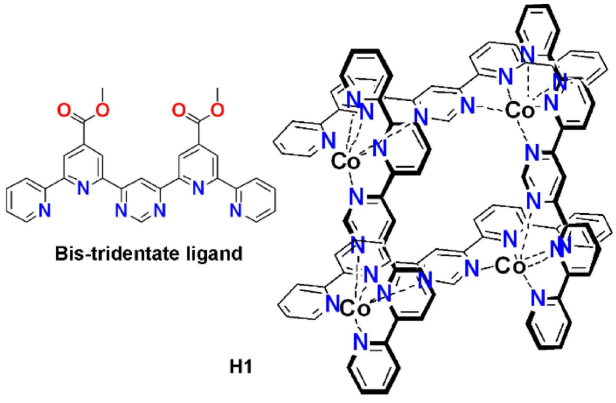

Scheme 4. $[M_4^{II}L_4]^{8+}$ [2 x 2] metal complex with Co(II) as central metal atoms and bis-tridentate ligands.

Stępień and co-workers synthesized zinc metallated π-extended porphyrin molecule conjugated with four naphthalenemonoimide moieties (NMI) (**H2**, Scheme 5).[51] This macrocyclic molecule can accumulate up to eight electrons by electrochemical and chemical methods. The electrochemical data of **H2** revealed eight reversible reduction waves from −0.97 V to −2.71 V vs Fc/Fc^+, each corresponding to one-electron reduction process. Chemical reduction of this macrocycle with sodium anthracenide under inert condition gives eight charged states showing red-shifted absorptions, extending beyond 2200 nm range in the optical spectrum. Additionally, the reduced state can again be transformed to its initial state by chemical oxidation with an excess of I_2 in approximately 90% yield.

Piraino and co-workers developed a multiredox active, dirhodium (II, II)-porphyrin-based molecular box (**H3**, Scheme 5).[52] This redox system was synthesized by combining $[Rh_2(form)_2(O2CCF_3)_2(H_2O)_2]$ (form = N,N′-di-p-tolylformamidinate) complex and meso-substituted phenylporphyrins in equimolar ratio. The CV analysis of **H3** revealed three oxidation waves at +0.53 V, +1.24 V and +1.60 V vs SCE, each wave consisting of four-electron oxidation process with one quasi-reversible reduction wave at −1.10 V for simultaneous four-electron reduction process. The first oxidation wave was assigned for four simultaneous Rh_2^{4+}/Rh_2^{5+} one-electron processes and the second wave were assigned for the oxidation of four porphyrin subunits, while the third oxidation wave for the four simultaneous Rh_2^{5+}/Rh_2^{6+} processes. The reduction peak was assigned to the four porphyrin centres, one-electron for each of the units.

Towards a hybrid multiredox system that utilizes Ru(II) ions, Zhong and co-workers synthesized a linear N–Ru–Ru–N system (**H4**, Scheme 5) consisting of two triarylamine sites connected by cyclometallated bisruthenium segment with a distance of 19.16 Å.[53] The CV and DPV results show four well-separated one electron oxidation waves at +0.38 V, +0.48 V, +0.83 V and +0.91 V vs Ag/AgCl. The starting two waves assigned for the oxidation of two distinct arylamine units and separation of 100 mV between two waves indicate electronic coupling between two distal amine units through the cyclometallated segment. Additionally, two one-electron reduction waves are also observed at −0.70 V and −1.14 V, associated with the reduction of central tetra-(2-pyridyl)pyrazine unit. Further, all the redox states were validated by spectroelectrochemical analysis.

Borovik et al., reported the synthesis of Fe(II) salt **H5** (Scheme 5), where the redox active ligand binds with the metal through the three anionic nitrogen, while the other coordination sites were occupied by 2,2′-bipyridine.[54] The complex **H5** exhibits attractive electronic properties with three oxidations at −0.94 V, −0.15 V, +0.60 V and one reduction at −2.09 V vs Fe/Fe^+. In addition, they also explored the catalytic activity of X towards the C–H activation of aryl azides at aliphatic and

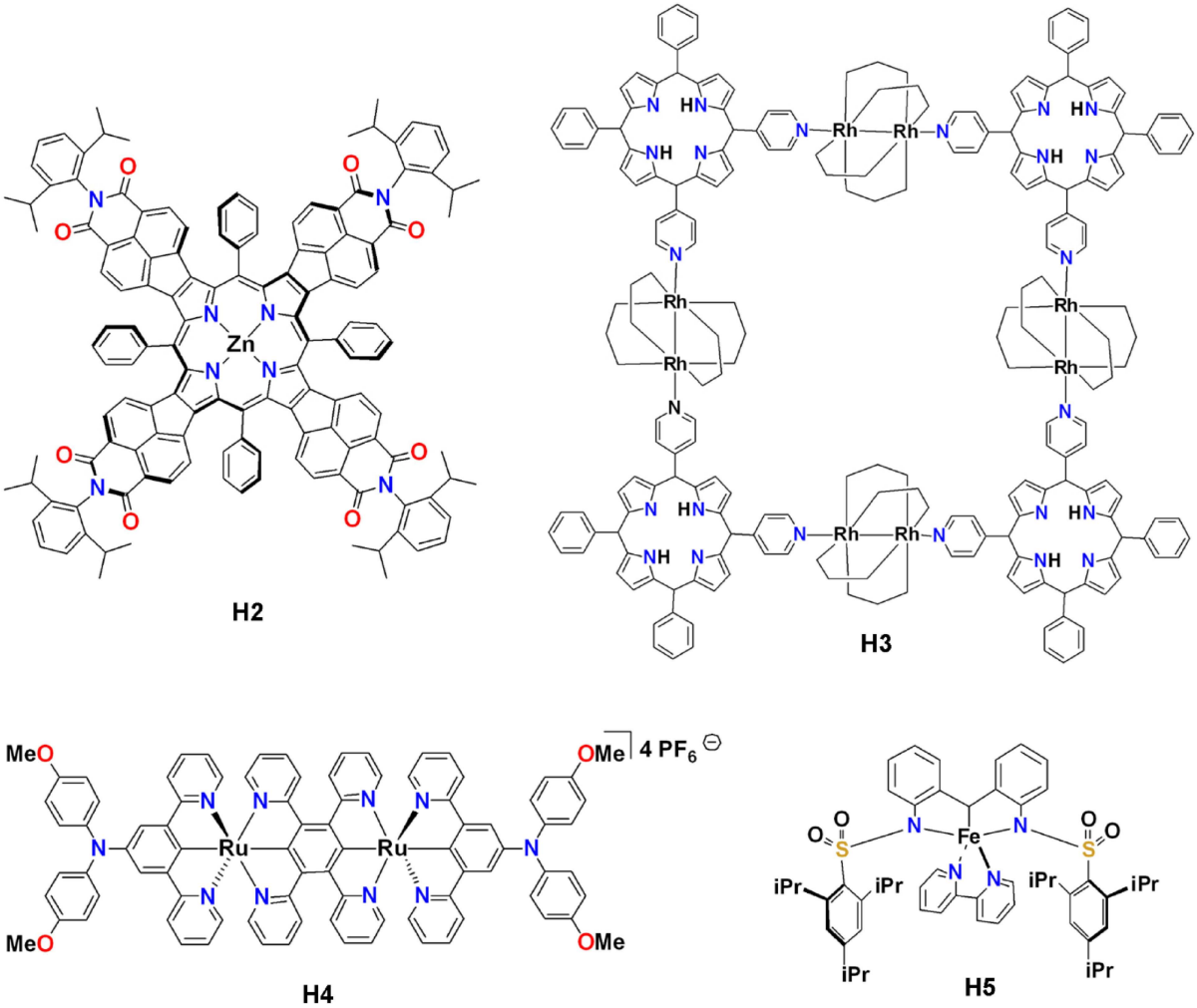

Scheme 5. Chemical structure of NMI conjugated Zn-porphyrin molecule **H2**, dirhodium (II, II)-porphyrin based square molecular box **H3,** Triphenylamine and bisruthenium-based linear array **H4,** Fe(II) salt **H5.**

benzylic carbon centres for intramolecular amination reaction, resulting in moderate to good yields of indoline products.

Würthner and co-workers reported a metallo-supramolecular self-assembled square box (**H6** Scheme 6) applying four perylene bispyridyl imide (PDI) as bridging ligands (each ligand have four ferrocene group at its bay position) and [Pt(dppp][$(OTf)_2$] as the corner units with an angle of 90° (dppp = 1,3-bis(diphenylphosphano)propane, OTf = trifluoromethanesulfonate).[55] This molecular box shows multi-redox properties due to the presence of 16 ferrocene units and four PDI scaffolds. The CV of **H6** exhibits two reversible reduction waves with $E_{1/2}$ at −1.01 V and −1.18 V vs Fc/Fc^+, each for four electrons indicating the reduction of four PDI units. One broad oxidation wave in the anodic region for the oxidation of 16 ferrocene units appears at −0.13 V with a shoulder at −0.08 V. Furthermore, this square box can also be chemically oxidized by utilizing thianthrenium pentachloroantimonate as oxidizing agent. The redox titration confirmed that all the ferrocene moieties could be oxidized and a highly charged species can be generated.

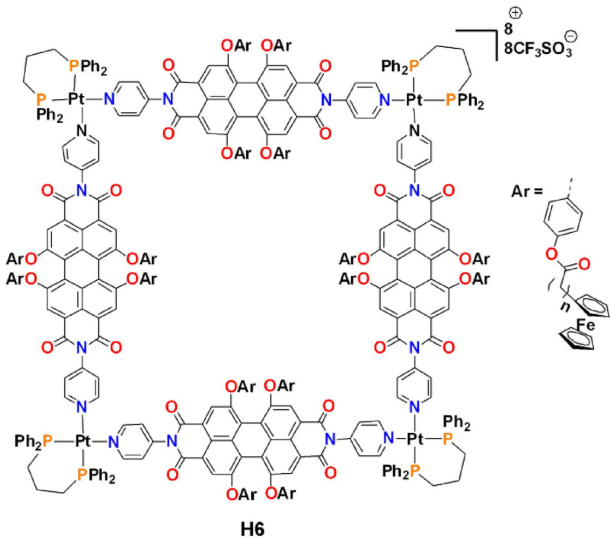

Scheme 6. Metallo-supramolecular square box **H6** containing 20 redox centres.

Dendritic branches have been applied as a novel platform to design multiredox hybrid systems. Astruc and his group reported a range of dendrimer molecules utilizing various redox active subunits, such as ferrocene, fullerene, etc.[56] In Scheme 7, we present a G1 generation dendrimer molecule having 27 termini ferrocenyl units **H7**.[57] They also synthesized a giant redox dendrimer of the G7 generation with 14000 termini ferrocenyl units. The CV analysis of the G7 generation molecule shows a single reversible redox wave, confirming that a large number of defects in such a giant molecule does not disturb their redox reversibility. Additionally, they confirmed the redox reversibility of these molecules by electrochemical and chemical methods.

Ishitani and his co-workers developed multinuclear ring-shaped metal complexes having six-redox active Re(I) units, **H8** (Scheme 8).[58] The electrochemical analysis shows a single peak at −1.68 V vs Ag/Ag+ for six-electron reduction processes each for one electron reduction of Re (I) metal, indicating absence of any electronic interactions between the two metal atoms. The six-electron reduced species is relatively stable in solution, although all the reduction steps need high potential (−1.68 V). Furthermore, this compound can also be reduced by the photochemical method in the presence of triethanolamine as donor compound and shows photochemical accumulation of 4.4 electrons in one molecule.

Sato and his co-workers reported a nona-nuclear copper grid metal complex (**H9**, Scheme 9), with the structural formula $[Cu_9^{II}(L)_6](BF_4)_6$, where L represents the 2,6-bis [5-(2-pyridinyl)-1H-pyrazol-3-yl] pyridine) ligand.[59] This metal complex shows multiredox property and CV analysis revealed four quasi-reversible redox waves each for one-electron transfer process at +0.44 V, +0.34 V, +0.09 V and −0.04 V vs SCE to form the $[Cu^{I}_4Cu^{II}_5]$ complex. The observation of four stepwise one-electron reductions indicates the existence of electronic coupling between neighboring metal ions.

They were also able to isolate two electron reduced species $[Cu^{I}_2Cu^{II}_7(L)_6](PF_6)_4$ and characterized it by single crystal X-Ray diffraction analysis.

Delgado and his co-workers reported vinylferrocenyl-functionalized cyclic and linear polysiloxanes with the structural formula $[MeSi\{C(Fc)=CH_2\}O]_4$ (**H10**) and (Me_3SiO)-$(MeSi\{C(Fc)=CH_2\}O)_n(SiMe_3)$ (**H11**, Scheme 10), where n is for approximately

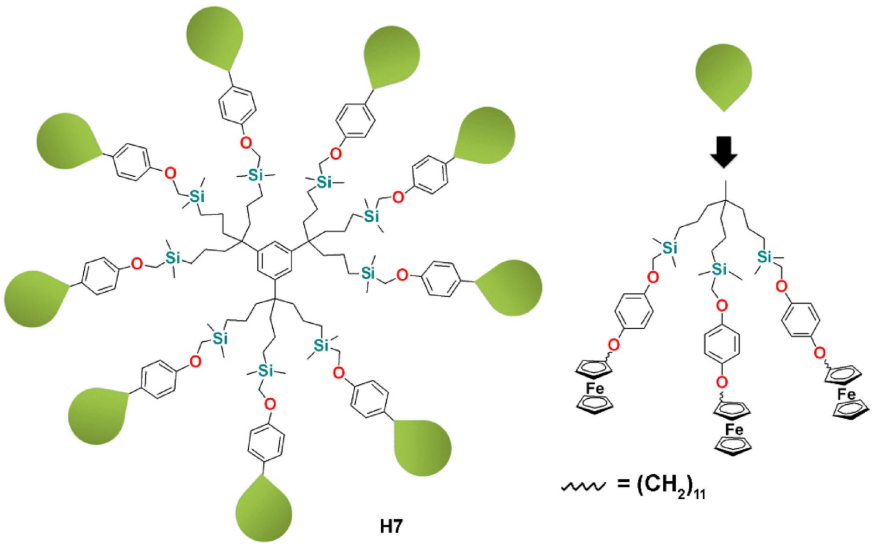

Scheme 7. Dendrimer molecule bearing 27 ferrocenyl redox units.

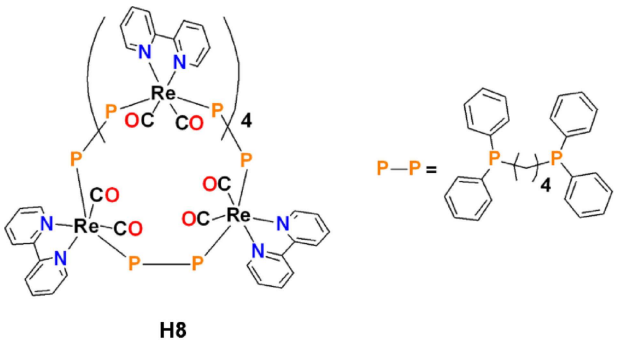

Scheme 8. Multinuclear ring-shaped multiredox system of Re(I) **H8.**

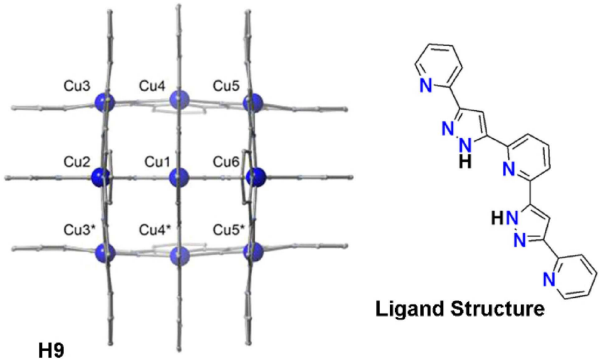

Scheme 9. Crystal structure of **H9**, $[Cu^{II}_9(L)_6](BF_4)_6$ based [3 x 3] metal grid and it's ligand structure.

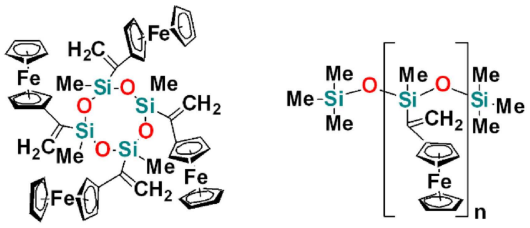

Scheme 10. . Molecular structure of vinylferrocenyl-functionalized cyclic (**H10**) and linear (**H11**) polysiloxanes

35 units and Fc represent the (η5-C_5H_4)Fe(η5-C_5H_5) unit.[60] In the electrochemical analysis, one reversible oxidation wave at +0.54 V vs SCE has been observed for both the cyclic and linear vinylferrocenyl-polysiloxanes associated with the Fe^{II}/Fe^{III} oxidation of ferrocenyl units. The presence of same oxidation pattern at same potential for both cyclic and linear molecule indicates that there is no electronic interaction between the two-neighboring pendant ferrocenyl groups along the polysiloxane backbones.

Cuadrado and co-workers have synthesized a carbosilane dendritic molecular system (**H12**, Scheme 11) bearing eight ferrocenyl units and twelve (η^6– aryl) tricarbonylchromium units.[61] This heterometallic dendritic molecule shows unique multiredox properties due to the presence of twenty redox-based metal centres. The DPV of compound **H12** shows two anodic peaks with $E_{1/2}$ value at +0.51 V and +0.91 V vs SCE and the integration of peak area shows the current ratio of 2:3 for the first and second peaks. The first oxidation peak is assigned to the simultaneous eight-electron oxidation process due to eight ferrocenyl subunits. The second broad peak for twelve-electron oxidation process is attributed to the electron removal from the twelve chromium centres. Broadening of the second peak is explained by the presence of two type of chromium centres, one is isolated (η^6-C_6H_5)$Cr(CO)_3$ unit linked to the Si-allyl group, while the other is in proximity to the already oxidized ferrocenyl moieties.

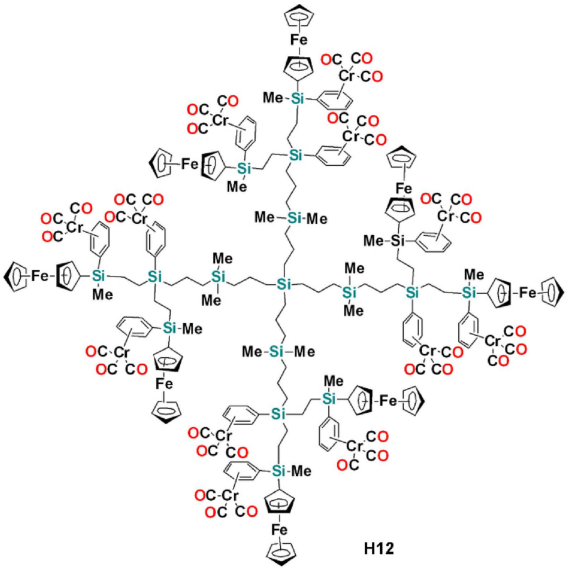

Scheme 11. Molecular structure of carbosilane dendritic system (**H12**) with twenty redox-based metal centres.

2.4. Supramolecular Multiredox Molecules

In a significant breakthrough in 1983, Hunig and co-workers reported the synthesis of various 4,4′-bipyridinium based-pyridinophanes.[62a] Application of the viologen unit in synthesis of new multiredox-active ionic boxes flourished with the isolation of the seminal '*blue-box*' by Stoddart and co-workers.[62b] Since then, a plethora of such highly electron-deficient boxes have been reported, which have been applied as charge-transfer materials, molecular switches and shuttles.[62c] In a leading-edge research, Stoddart et al., reported a highly charged octa-cationic homo[2]catenane **SM1** by using two cyclobis(paraquat-p-phenylene) rings (Scheme 12). They showed that this system is capable of taking eight-electrons among which six-redox states could be electrochemically accessed.[62d]

Stoddart et al., synthesized the viologen-based extended cyclophane (**SM2**), which has been employed as a C_{60} receptor.[63] The 1:1 inclusion complex of **SM2** and C_{60} displayed columnar self-assembly (Figure 1). The electrochemical analysis showed multiredox behaviour with minor shifts in reduction potentials of each of the components in 1:1 complex as compared to unbound **SM2** and C_{60}. The most observable change was found in the first reduction, where E^1_{red} for the 1:1 complex was observed at −0.31 V compared to −0.34 V vs Ag/AgCl for free C_{60}.

In another report, Stoddart and co-workers synthesized thermal and photo-responsive semi-rigid multiredox rectangular cyclophane **SM3** (Scheme 13), consisting of biphenylene-bridged 4,4-bipyridinium and oligo(*p*-phenylenevinylene) pyridinium extended viologens.[64] The oligo(*p*-phenylenevinylene) pyridinium unit were incorporated to alter the macrocycle configuration between (EE)- and (EZ)- isomers upon heating and blue-light irradiation. When **SM3** is found in (EE)-configuration, it has potential to bind various electron-rich and electron-deficient π-guests through van der Waals and charge

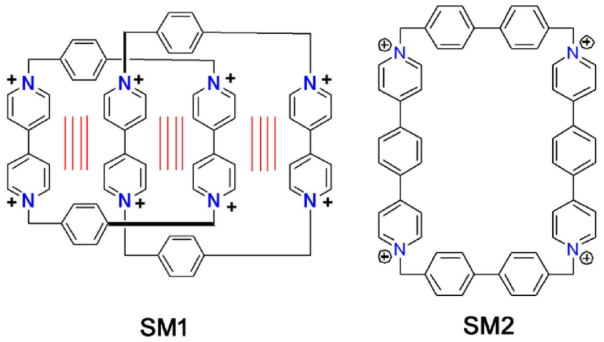

Scheme 12. Molecular structures of octa-cationic homo[2]catenane **SM1** and extended cyclophane **SM2**.

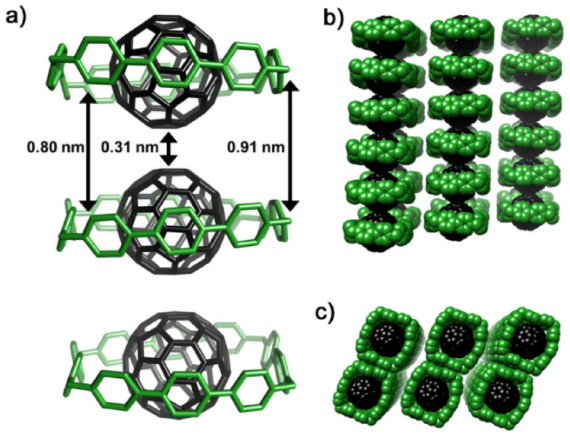

Figure 1. Crystal structure of **SM2**:C_{60} complex; a fullerene-to-fullerene distance of 0.31 nm between the aligned C60 molecules (a), The side-on view (b) and plan view (c) of the solid-state superstructure illustrate the close packing arrangement. Reprinted with permission from 63. Copyright 2015 American Chemical Society.

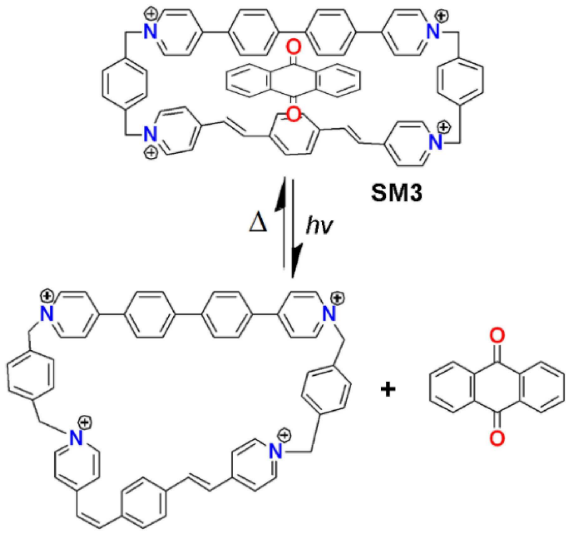

Scheme 13. Photoswitchable molecular encapsulation of dynamic tetracationic cyclophane.

transfer interactions. Upon irradiation with blue light the (EE)-isomer of **SM3** converted to EZ isomers, which results in the switching off the binding affinity of the guest molecules. The process can be reversed upon heating.

In another report, synthesis of '*blue-box*' based daisy chain containing viologen and 1,5-dioxynaphthalene units were reported by Stoddart and co-workers. This daisy chain was converted to mechanically interlocked self-complementary assemblies by stoppering process, out of which one representative example (**SM4**) is presented here (Figure 2).[65] Interestingly, the position of '*blue-box*' has been electrochemically switched between viologen and dioxynaphthalene units, by utilizing spin- pairing and donor-acceptor interactions, respectively. The CV revealed the first six-electron reduction peak at −0.32 V to generate two tris-radical viologen ($^{\bullet}+$) – '*blue-box*' ($^{\bullet}+$) sub-complexes. Other two reduction peaks were found at −0.74 V ($2e^-$) and −1.03 V ($1e^-$) vs Ag/AgCl for the formation of completely neutral complex.

In a recent report, Stoddart group demonstrated host-guest interactions between an extended molecular-box and NDI to construct mechanically interlocked [2]catenane (**SM5**), where the NDI unit can be encapsulated inside the molecular box (Scheme 14).[66a] It was found that redox properties of the NDI can be modified significantly, and its reduction was facilitated due to the coulombic attraction with tetracationic ring. Importantly, the viologen cyclophane stabilizes the NDI radical anion and also forms the NDI^{2-} dianion upon further reduction. In this context, the first NDI radical ion was stabilized and isolated by integrating two phosphonium groups at the NDI-core, which forms two P–O through space donor-acceptor type non-covalent interactions.[66b]

In an innovative development, Stoddart and co-workers reported the encapsulation of the mechanically interlocked bistable molecule (**SM6**) inside the robust zirconium-based metal-organic framework (MOF), NU-1000, by using the post-synthetic modification (Scheme 14).[67] They found that two **SM6** units can be integrated in one repeating unit of hexagonal channels of MOF NU-1000. The electrochemical and optical analysis demonstrated that **SM6** retains its reversible redox-switching behaviour even inside the nanopores of the MOF.

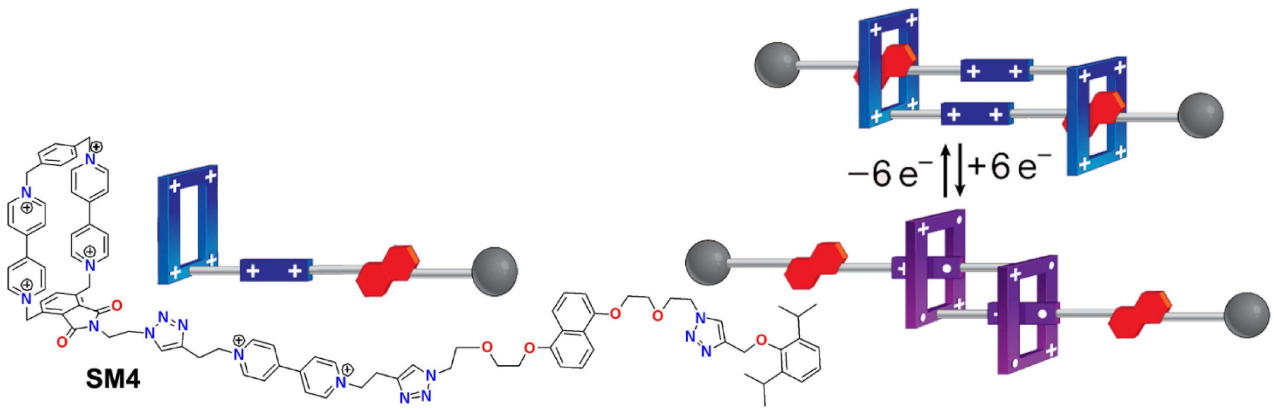

Figure 2. Structure of daisy chains **SM4** and representation of redox switchable rotaxene controlled by the radical-radical interaction.

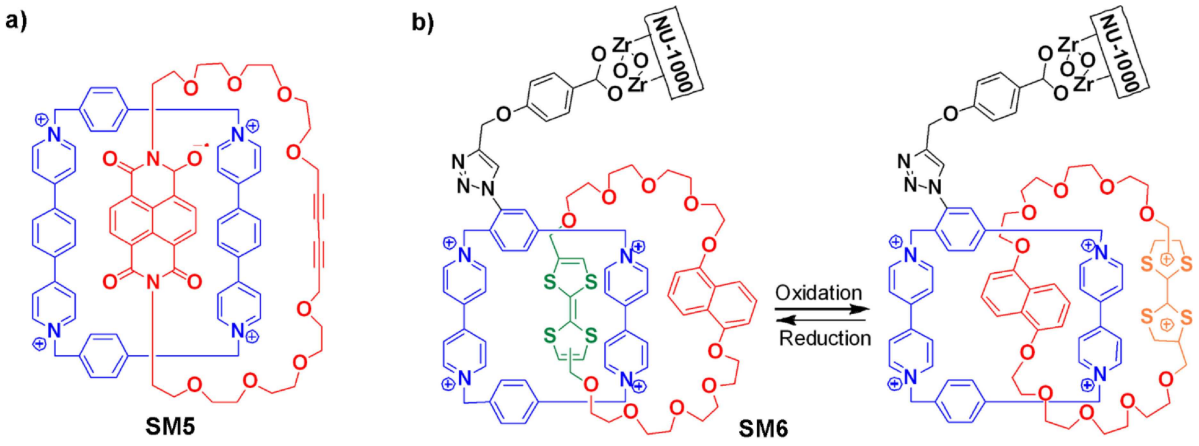

Scheme 14. Stabilization of NDI radical anion within the cyclophane (a), redox-switchable bistable catenane (b).

Sessler and co-workers reported an novel multiredox system with switchable properties. They reported the synthesis of the multiredox active host-guest complex of tetrathiafulvalene calix [4]pyrrole **SM7** donor and the bisimidazolium quinone **SM8** as an acceptor (Figure 3).[68] It was demonstrated that some specific anion such as methylsulfate, chloride and bromide to have strong binding with donor unit **SM7**. This results in a significant change in the host conformation, which facilitates the electron transfer from **SM7** to **SM8** for the formation of **SM10** and **SM11** through a proposed intermediate **SM9**. The electron transfer reaction could be made reversible by addition of tetraethylammoniumchloride (TEACl).

3. Application of Multiredox Materials

3.1. Photochemical Accumulation in Artificial Photosynthesis

Photosynthesis is one of the well-known multielectron redox-based biological processes, which converts sunlight into chemical energy by utilizing water and CO_2. In green plants, light dependent reactions proceed in chloroplasts (thylakoid membranes).[5] This process has two complementary reaction centres photosystem-I (PS-I) and photosystem-II (PS-II) (Figure 4), which utilize electron transport chain to produce NADPH as a main reducing agent which works as a source of energetic electrons for other cellular reactions. For this process, water works as an electron source; two water molecules split into diatomic oxygen, four proton and four electrons, the produced electrons transferred to oxidized PS-II centres of the chloroplast. The overall equation of the light-dependent reaction of photosynthesis is as follows:

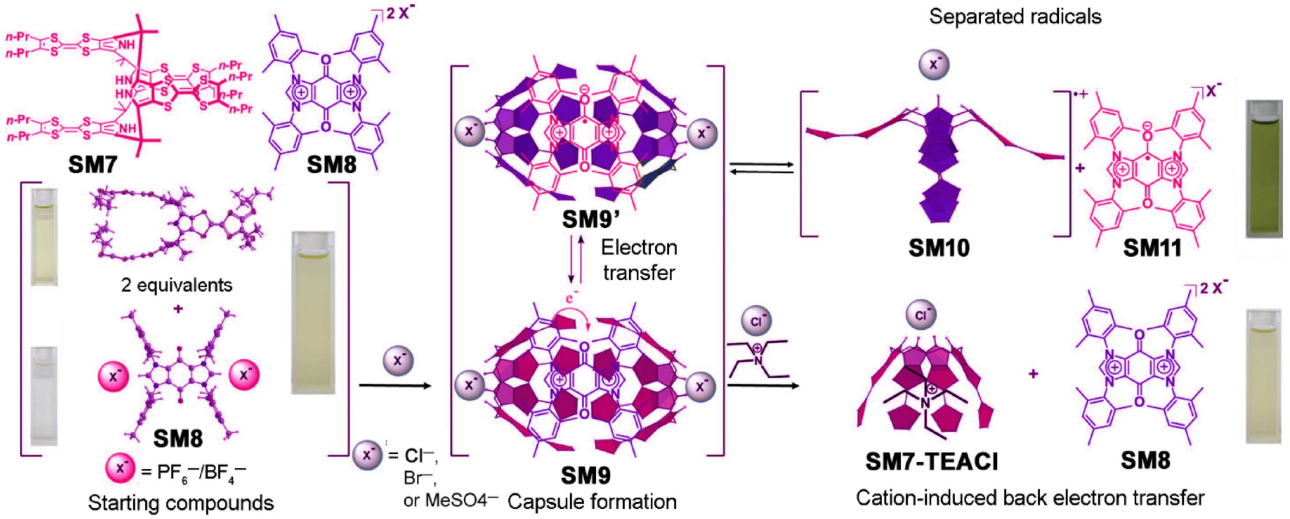

Figure 3. Chemical structures of **SM7**, **SM8** and their ion mediated electron transfer reaction.

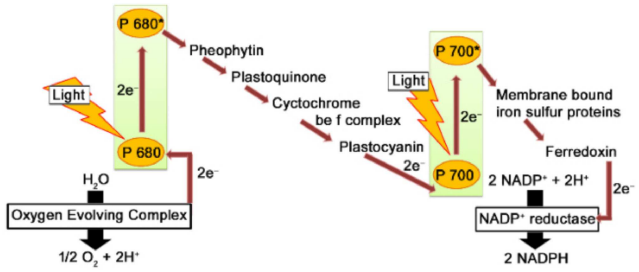

Figure 4. Schematic diagram of multi-electron transfer based light dependent photosynthesis reactions (Z-scheme).

$$2\ H_2O + 2\ NADP^+ + 3\ ADP + 3P_i + light \rightarrow 2NADPH + 2\ H^+ + 3\ ATP + O_2 \quad (1)$$

Molecular dyes and semiconducting materials have been utilized in photovoltaic cells for a long time. Scientists are trying to develop artificial systems for light harvesting application in advanced solar fuel production. Direct conversion of solar energy into fuel energy can satisfy our future large-scale energy demands. Solar fuels can be produced, by absorption of light and direct conversion of its energy to chemical energy by electron transfer processes.[69] When a single photon is absorbed, it directs the separation of a single electron-hole pair. These electrons can be utilized in the catalytic reduction of water like cheap low energy content substrate into high energy fuel. The holes are filled by electrons generated by water oxidation.[70] Basically, fuel production and water oxidation processes are multi-electron and multi-proton in nature. Therefore, after absorption of several photons, a system must be able to accumulate multiple holes and electrons to complete the catalytic reaction, before the charge recombination occurs. These catalytic reactions require multiple redox equivalents and their coupling to proton transfer reactions.[71] For the light harvesting and charge separation; scientists are trying to develop new multiredox active systems, which are better optimized than those used in the earlier devices for solar fuel production. In addition, there is significant progress in the design and discovery of hetero and homogeneous catalysts for water oxidation and solar fuel production.[72]

Hammarström in his account represented schematically catalytic solar fuel production.[73] As shown in Figure 5, an antenna (Ant) molecule absorbs a photon and transfers its excitation energy to photosensitizer (P). This photosensitizer transfers a hole and an electron to the donor (D) and acceptor (A) unit, respectively. The separated electrons and holes are accumulated on catalysts (CAT). On one catalyst, the redox equivalents are used to split the water molecule into dioxygen molecule. While on the other catalyst substrate, like protons or carbon dioxide are reduced into fuel, which could be hydrogen, an alcohol or carbon containing materials. The two-compartment system is required to avoid the interaction of generated fuel such as H_2, CO and methane with oxygen molecules. In conclusion, to assemble a completely photocatalytic system, we require precisely designed molecular systems having controlled electronic properties and interactions.

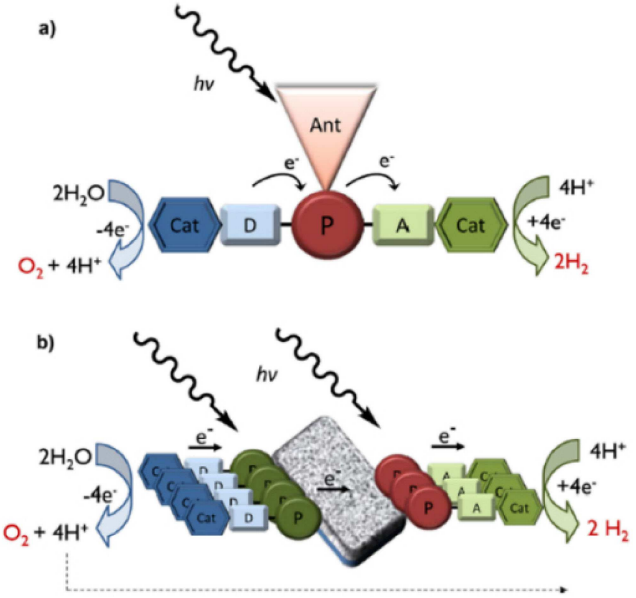

Figure 5. (a) Schematic diagram of a molecular system for conversion of solar energy into fuel by light-induced charge separation coupled with water oxidation and catalytic fuel production. (b) Schematic representation of two-compartment system connected by charge transport material as loose redox-pool. Reprinted with permission from 73. Copyright 2015 American Chemical Society.

3.2. In Water Splitting Reaction

Natural energy sources are coming into use as sustainable, clean and renewable energy sources, but because of their unstable output and the difficulty in large-scale electricity storage, these sources are incapable of meeting the high energy demands. In green plants, photosynthesis process converts the solar energy into chemical energy and stores it in the form of carbohydrates. In a similar way, if the natural energy can be converted into chemical bonding energy, then it can be a promising approach to enable the facile energy storage and transportation.[74] As we know hydrogen gas is one of the well-known energy storage systems because of its high energy density and clean combustion. Therefore, water splitting into H_2 and O_2 by photochemical or electrochemical processes is growing great attention. The two half reactions of water splitting are as follows:

$$2H^+ + 2e^- \rightarrow H_2\ (E^\circ = 0.00\,V\ vs\ SHE\ at\ pH\,0) \quad (2)$$

$$2H_2O \rightarrow O_2 + 4H^+ + 4e^-\ (E^\circ = 1.23\,V\ vs\ SHE\ at\ pH\,0) \quad (3)$$

The major difficulty associated with electrochemical water splitting process is anodic oxidation reaction (eq. 3), in which two water molecules combine to give O–O bond and release four electrons and four protons. Therefore, for processing of these four successive one electron oxidation steps, the rational design and synthesis of molecular catalysts is essential to achieve water oxidation reaction near the thermodynamic limits (E = 1.23 V).[75] In photosystem-II, this difficult reaction proceeds

by a molecular catalyst working as an oxygen evolving complex (OEC), which is a tiny metal oxide (Mn_4CaO_5) composed of four manganese ions, one calcium ion and five oxygen atoms. This complex can adopt five successive oxidation states by the redox reaction of the Mn ions. This natural OEC system has inspired synthetic chemists to mimic catalytic system for artificial photosynthesis. In last three decades, many multinuclear transition metals, such as ruthenium (Ru) and manganese (Mn) based molecular catalyst have been synthesized for water splitting application.

Meyer et, al., reported polypyridyl dinuclear ruthenium complex (**1**), as one of the first homogeneous oxygen evolving molecular catalyst in 1982 called as '*blue-dimer*'.[76] In the presence of an excess amount of oxidants such as Co^{III} and $(NH_4)_2[Ce^{IV}(NO_3)_6]$ (CAN) the '*blue-dimer*' evolves oxygen gas in 87% yield with 13.2 turnover number (TON).[77] Following this discovery, Naruta and co-workers reported the first example of a Mn-based homogeneous molecular catalyst (**2**, Scheme 15) in 1994.[78] Electrolysis of Mn porphyrin dimer shows the potential window of +1.2 to +2.0 V (vs. Ag/Ag^+) which results in the O_2 gas evolution with 5–17% current efficiency and 9.2 TON. Sun and co-workers have reported extremely active oxygen evolving Ru complex (**3**), in 2012.[79] In the presence of CAN; complex **3** evolved O_2 with as high as 55400 TON. After applying it as an electrochemical catalyst, they also functionalized these Ru-based catalysts for photocatalytic water splitting by depositing the material onto a TiO_2-modified fluorine-doped tin oxide (FTO) electrode in which the $[Ru(bipy)_3]$ derivatives function as the photosensitizer with approximately 500 TON with an external bias of (0.2 V).[80]

3.3. In Advanced Power Storage Systems

To power today's world, electrochemical batteries are proven as efficient and simple power storage systems. However, most of these existing power storage systems utilize heavy metal oxides with single or less than one- electron redox properties.[81] Therefore, these systems are not sufficient to accomplish the increasing demand for future portable electronics. Consequently, to greatly enhance the power capability and energy storage density of batteries, there is an urgent need for a realistic breakthrough in battery technology. In recent years, some newly designed battery materials have been demonstrated, utilizing the concept of light molecular weight and multiredox active electrode material.[82]

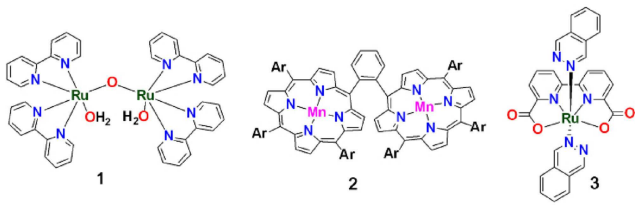

Scheme 15. Molecular structures of reported water-splitting catalyst (**1**-**3**).

The specific energy density (ED) of a battery system can be calculated from the following equation:

$$ED = \frac{nFE^{\circ}}{\sum Mi}$$

The unit of ED can be expressed either in the term of per unit of volume ($Wh\,L^{-1}$) or per unit of weight ($Wh\,kg^{-1}$). Here, n represents the number of electrons transferred per mole of reactants, F stands for the Faraday constant. E° refers the electromotive force (emf) of the cell reaction. ΣMi the sum of the molecular weight of active material being transformed in the cell reaction called as redox drivers. Therefore, in order to construct advanced batteries systems with high energy density, the electrode of batteries must have these properties: (a) there should be a large potential difference between the anode and cathode active material to produce higher voltage, (b) multiple electrons transferred per molecule and (c) the lighter molecular weight of the active materials.

Hence, for the construction of high energy density batteries, the electroactive materials should be chosen with light molecular weight. From the above equation, we can say that the utilization of multiredox active materials may work as the most effective tool to build up the high energy density power storage systems. Additionally, organic electroactive materials are becoming more desirable, due to their, structural diversity, resource sustainability, electrochemical performance, flexibility and eco-friendly behaviour.[83] Particularly, molecules containing carbonyl groups have attracted great attention due to their multiredox active nature and the abundance of natural products. The molecules containing carboxylates, quinones, anhydride and imides have been successfully utilized in rechargeable lithium batteries.[84]

Recently, Yao et al. investigated 2,5-dimethoxy-1,4-benzoquinone (DMBQ) as a positive electrode active material for rechargeable lithium batteries.[85] This positive electrode showed stepwise two-electron redox property and the initial discharge capacity of this battery reported as 312 $m\,Ahg^{-1}$ with an average voltage of 2.6 V vs Li+/Li and fair cyclic behaviour (Figure 6). Because of the two-electron redox behaviour the discharge capacity of this battery is more than two times than that of the conventional lithium cobalt oxide ($LiCoO_2$) electrode material.

3.4. In Dynamics Random Access Memory

Dynamics random access memory (DRAM) works as the central memory element in various devices, such as laptop, computer and standard desktop. The high memory density of DRAM,

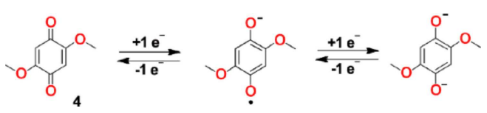

Figure 6. Representation of two electrons redox behaviour of dimethoxy-benzoquinone.

because of its small size, gives it more advancement over the other memory technologies like static random-access memory. The small size DRAM is due to its basic cell, which consist of one capacitor and a transistor.[86,87]

For having high memory density, the capacitor needs to store at multibit level. For featuring a system in DRAM, it should have at least three distinct cationic redox states.[88] For getting the multiredox states at distinct potential, there are two types of approaches generally applied. One is the use of the mixture of redox active molecules, while the second approach incorporates the utilization of multiredox active single molecule. For the construction of hybrid semiconductor/molecular DRAM, the basic approach is the use of redox-active molecule which is covalently bonded to an electroactive surface. The information is stored in the distinct redox state of the molecule. The composition of charge storage molecule decides the charge density, voltage, stability and size. On the other hand, the composition of surface attaching group defines the charge storage rate and charge retention time.

A molecular system should possess the following properties to be applied in DRAM system: (1) The various redox states of the molecule should be stable under ambient condition, which is important for the real-world application. (2) For affording multibit information with low power consumption, the molecules should exhibit multiple redox states at relatively low potential. (3) They should be able to store charge for minutes in the absence of applied potential; this will further diminish the power consumption and appreciably attenuate the refresh rate needed in a memory device.

Lindsey group reported a porphyrin-based charge-storage memory system. They have chosen porphyrin molecule because on its specific, robust electronic properties, which provides the basis for writing and reading the memory cell. Figure 7 shows the read/write strategy for the porphyrin-based memory system. As shown in Figure 7b, monomeric Zn porphyrin exhibits two distinct cationic states. The oxidation of the neutral molecules to mono-cationic radical ion constitutes writing of a bit of information. Subsequently, the reduction of mono-cation to neutral state constitutes reading out the information.

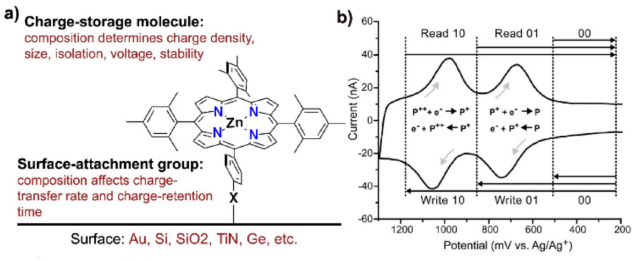

Figure 7. (a) Representation of porphyrin-based memory element, (b) redox-based read and write process. P represents porphyrin.

3.5. As Catalyst in Multi-electron Transfer Reactions

Transition-metal complexes are critical components to mediate multi-electron transformations of various small molecules. Such as the reduction of the proton to H_2 and oxidation of C–H bonds are both two-electron transformations.[89,90] Water oxidation is a four-electron reaction[91] while the reduction of nitrogen to transform into ammonia is a six-electron process.[92] The design of catalytic material for these transformations requires the utilization of one or two metal atom with a variable valency. Incorporation of multiredox active ligands in the metal coordination sphere can work as an alternative route for supplying the oxidizing and reducing equivalents.[93] For example, Zarkesh et al., have proposed a new strategy for the design of metal complex based catalytic material for the multi-electron redox reaction. They have reported the use of tridentate redox-active ligand $[ONO^{red}]^{3-}$ coordinated with tantalum (**5**, Figure 8) as a catalytic material for four electron transformation of aryl diazenes.[94] This bridging imido dimer gives aryl diazene in equimolar ratio and requires the use of two equivalent of $PhICl_2$. The important aspect of this catalysis reaction is the role of redox active ligand $[ONO^{red}]^{3-}$, as this ligand can be oxidized to the dianionic semi-quinonate ligand, or trianionic quinonate ligand. The oxidation states of this ligand could store single-electron oxidizing equivalents earlier to the elimination of aryl diazene.

In another example of multi-electron transfer reaction, conversionof hydrazines into azo molecules proceeds by the two-electron transfer process. This reaction is important, as azo compounds are useful in materials and electronic applications. To catalyze this reaction metal complex with two-electron valance states is required. Blackmore et al., have reported a new type of catalyst $[N_2O_2^{red}]Zr[THF]_3$ having Zr° with multiredox active ligand $[N_2O_2^{red}]^{4-}$ (**6**, Figure 8), for the disproportionation reaction of diphenylhydrazine to azobenzene and aniline.[95] This catalytic reaction proceeds by change in the redox state of the multiredox active ligand rather than the metal centre.

$$2PhHN{-}NHPh \rightarrow PhN = NPh + 2NH_2Ph$$

They were also able to implicate the intermediate state with two electrons oxidized ligand $[N_2O_2ox]_2$–Zr-imido. The electronic properties of the metal centre coupled with the redox properties of ligand enable to catalyze the electron transfer reaction.

3.6. In Electrochemical Biological Sensor

Clinical diagnosis needs the advanced biosensor technologies for highly sensitive and specific detection of biomolecules and their interaction. The most common analytical technologies used for biomolecule detection is calorimetry, fluorescence spectroscopy, surface-plasmon-resonance and quartz crystal microbalance. Generally, these techniques need the use of the fluorophore, bio-label for getting the measurable signal.[96] The development of electrochemical method as the biosensor is

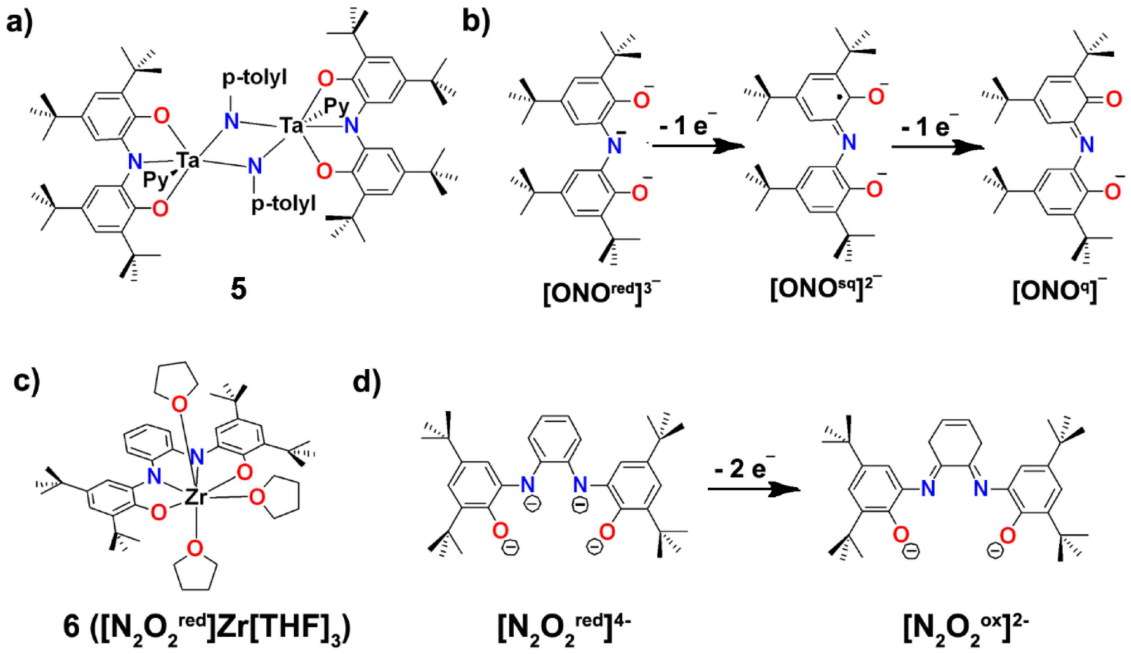

Figure 8. (a) Metal complex **5** as a catalytic material with tridentate redox active ligand, (b) various redox states of the ligand of complex **5**, (c) catalyst (**6**) consist of Zr° metal and active redox ligand, and (d) redox reaction of the ligand of complex **6**.

receiving great attention because of their low cost, high sensitivity and can work even in turbid media. In the electrochemical method, the signal intensity can be enhanced by increasing the surface area of the electrode, and by utilization of the multiredox active signaling probe.[97,98]

Based on these ideas Li et al., have reported an electrochemical DNA sensing method, applying capture probe-target-signaling probe (CP–T–SP).[99] Applying the multiredox active signaling probe dramatically improved the sensitivity by increasing the detection limit of the current signal. The sensor can detect target DNA at an extremely low concentration of 2 fm with good mismatch discrimination ability. These DNA sensors have the capability to work in real complex matrixes, such as whole blood and serum.

In another example, mannose-ferrocene conjugates based electrochemical probe have been developed for the detection of lectin Concanavalin A (Con A) protein.[100] Most of the important biological processes such as bacterial and viral infection, inflammatory and immune response, cell-cell adhesion, fertilization and cancer metastasis are governed by the carbohydrates and protein interactions. To improve the recognition ability of carbohydrate-lectin interaction, Berenguel and co-workers designed the signaling probe with multivalent dendritic glycoside labeled with redox-active ferrocene moieties (Figure 9). They reported electroactive poly(amido amine) based glycodendrimer of G0 to G2 generation having mannopyranosyl-ferrocenyl moieties at the periphery. These multiredox active dendrimers showed an enhanced affinity for Con A as compared to mono and divalent analogues due to the multivalent effect. This behaviour is attributed to the effect of multielectron exchange due to the presence of dendritic ferrocene and multivalent binding interaction of glycoside.

4. Conclusion

Through this review, we have highlighted the diverse molecular design that has led to the realization of different multiredox molecules and supramolecular systems. The multiredox systems reviewed here can perform at least four-electron transfer processes. Firstly, we have classified the molecular multiredox systems into organic and organic-inorganic hybrid systems. The organic multiredox systems are further classified into multielectron acceptors, multielectron donors and ambipolar molecules. Further, we have reviewed supramolecular multiredox systems, redox-active host-guest recognition, including mechanically interlocked systems. Finally, the review provides a discussion on the diverse applications, e.g. in artificial photosynthesis, water splitting, dynamic random-access memory, etc. that can be realized from these artificial multiredox systems. As can be appreciated, artificial multiredox systems have the potential to provide solution to the present energy needs. These can as well offer deeper understanding of the various multielectron-based processes in biological systems. Also, important are the multifaceted organic radicals and radical ions that are the usual by-products of multielectron-based processes.[101]

Acknowledgements

PM thanks financial support under SwarnaJayanti Fellowship (DST/SJF-02/CSA-02/2013-14), DST-FIST and DST-PURSE. PM thanks SPS, JNU and AIRF, JNU which provided crucial infrastructural support over the years. The important contribution of former research scholars: Dr. M. R. Ajayakumar, Dr. Deepak

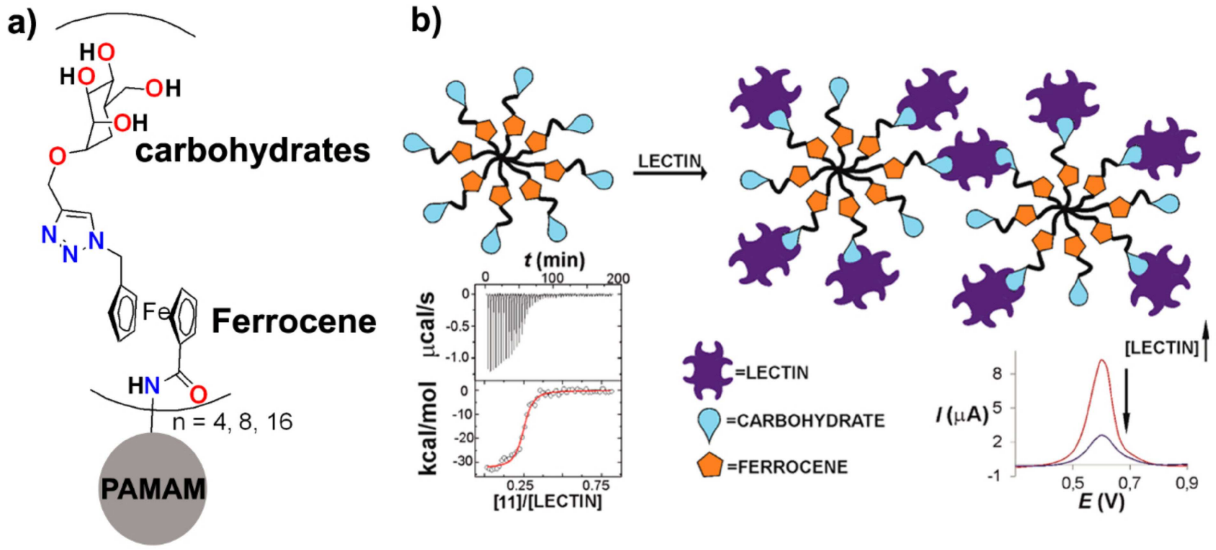

Figure 9. Chemical structure of mannose-ferrocene conjugates based electrochemical probe (a), and schematic representation of carbohydrates and protein interactions (b). Reprinted with permission from Ref. 100. Copyright 2013 American Chemical Society.

Asthana, Dr. Srikanta Dana, Dr. Sudhir Kumar Keshri, Dr. Sharvan Kumar, Dr. Kalyanashis Mandal and Dr. Yogendra Kumar towards carrying out some of the outlined research from our group are greatly acknowledged.

Keywords: supramolecular multiredox systems · organic multielectron acceptor · organic multielectron donor · organic–inorganic hybrids · energy storage materials

[1] a) *Supramolecular Chemistry: Concepts and Perspectives*, J.-M. Lehn, VCH, Weinheim **1995**; b) J.-M. Lehn, *Science* **2002**, *295*, 2400–2403; c) K. Eda, T. Osakai, *Inorg. Chem.* **2015**, *54*, 2793–2801.
[2] a) E. Palecek, *Anal. Biochem.* **1988**, *170*, 421–431.
[3] a) S. Weber, *Biochim. Biophys. Acta.* **2005**, *1707*, 1–23; b) J. Strumpfer, M. Sener, K. Schulten, *J. Phys. Chem. Lett.* **2012**, *3*, 536–542; c) Z. Zhang, L. Huang, V. M. Shulmeister, Y. I. Chi, K. K. Kim, L. W. Hung, A. R. Crofts, E. A. Berry, S. H. Kim, *Nature* **1998**, *392*, 677–684.
[4] a) G. Armendariz-Vidales, L. S. Hernandez-Munoz, F. J. Gonzale, A. A. De Souza, F. C. De Abreu, G. A. M. Jardim, E. N. Da Silva, M. O. F. Goulart, C. Frontana, *J. Org. Chem.* **2014**, *79*, 5201–5208; b) L. Ciofini, T. L. Bahers, C. A. Adaneo, F. Odobel, D. Jaccquemin, *J. Phys. Chem. C* **2012**, *116*, 11470–11479.
[5] P. H. Raven, R. F. Evert, S. E. Eichhorn, *Biol. Plant.* **2005**, *7*, 124.
[6] a) S. O. Obare, T. Ito, G. J. Meyer, *J. Am. Chem. Soc.* **2006**, *128*, 712–713; b) H. H. Mohamed, C. B. Mendive, R. Dillert, D. W. Bahnemann, *J. Phys. Chem. A* **2011**, *115*, 2139–2147; c) A. Volpe, A. Sartorel, C. Tubaro, L. Meneghini, M. Di Valentin, C. Graiff, M. Bonchio, *Eur. J. Inorg. Chem.* **2014**, 665–675.
[7] a) D. Gust, T. A. Moore, A. L. Moore, *Acc. Chem. Res.* **1993**, *26*, 198–205; b) D. V. Yandulov, R. R. Schrock, *Science* **2003**, *301*, 76–78; c) K. Rajeshwar, C. Janaky, W. Y. Lin, D. A. Roberts, W. Wampler, *J. Phys. Chem. Lett.* **2013**, *4*, 3468–3478; d) M. R. Wasielewski, *J. Org. Chem.* **2006**, *71*, 5051–5066; e) S. R. Greenfield, W. A. Svec, D. Gosztola, M. R. Wasielewski, *J. Am. Chem. Soc.* **1996**, *118*, 6767–6777; f) R. Bhosale, R. S. K. Kishore, V. Ravikumar, O. Kel, E. Vauthey, N. Sakai, S. Matile, *Chem. Sci.* **2010**, *1*, 357–368; g) N. Sakai, A. L. Sisson, T. Bürgi, S. Matile, *J. Am. Chem. Soc.* **2007**, *129*, 15758–15759; h) C. Röger, Y. Miloslavina, D. Brunner, A. R. Holzwarth, F. Würthner, *J. Am. Chem. Soc.* **2008**, *130*, 5929–5939; i) C. Röger, M. G. Müller, M. Lysetska, Y. Miloslavina, A. R. Holzwarth, F. Würthner, *J. Am. Chem. Soc.* **2006**, *128*, 6542–6543.
[8] a) J.-L. Fillaut, J. Linares, J. Astruc, *Angew. Chem. Int. Ed. Engl.* **1994**, *33*, 2460–2462; b) C. Lambert, G. Noll, *Angew. Chem. Int. Ed. Engl.* **1998**, *37*, 2107–2110; c) S. C. Blackstock, T. D. Selby, *J. Am. Chem. Soc.* **1998**, *120*, 12155–12156.
[9] a) F. W. Wassmundt, W. F. Kiesman, *J. Org. Chem.* **1995**, *6*, 1713–1719; b) G. Hautier, A. Jain, T. Mueller, C. Moore, S. P. Ong, G. Ceder, *Chem. Mater.* **2013**, *25*, 2064–2074.
[10] a) I. V. Kuvychko, K. P. Castro, S. H. M. Deng, X.-B. Wang, S. H. Strauss, O. V. Boltalina, *Angew. Chem. Int. Ed.* **2013**, *52*, 4871–4874; *Angew. Chem.* **2013**, *125*, 4971–4974; b) P. E. Hartnett, A. Timalsina, H. S. S. R. Matte, N. Zhou, X. Guo, W. Zhao, A. Facchetti, R. P. H. Chang, M. C. Hersam, M. R. Wasielewski, T. J. Marks, *J. Am. Chem. Soc.* **2014**, *136*, 16345–16356.
[11] a) S. Kumar, P. Mukhopadhyay, *Green Chem.* **2018**, *20*, 4620–4628; b) Y. Kumar, S. Kumar, K. Mandal, P. Mukhopadhyay, *Angew. Chem. Int. Ed.* **2018**, *57*, 16318–16322; c) S. Kumar, J. Shukla, Y. Kumar, P. Mukhopadhyay, *Org. Chem. Front.* **2018**, *5*, 2254–2276.
[12] Q. Xie, E. Perez-Cordero, L. Echegoyen, *J. Am. Chem. Soc.* **1992**, *114*, 3977–3978.
[13] a) P. M. Allemand, K. C. Khemani, A. Koch, F. Wudl, K. Holczer, S. Donovan, G. Gruner, J. D. Thompson, *Science* **1991**, *253*, 301–302; b) K. Holczer, O. Klein, S. Huang, R. B. Kaner, K. J. Fu, R. Whetten, F. Diederich, *Science* **1991**, *252*, 1154–1157; c) G. Dennler, M. C. Scharber, C. J. Brabec, *Adv. Mater.* **2009**, *21*, 1323–1338; d) M. Carano, T. D. Ros, M. Fanti, K. Kordatos, M. Marcaccio, F. Paolucci, M. Prato, S. Roffia, F. Zerbetto, *J. Am. Chem. Soc.* **2003**, *125*, 7139–7144.
[14] A. C. Benniston, J. Hagon, X. He, S. Yang, R. W. Harrington, *Org. Lett.* **2012**, *14*, 506–509.
[15] G. B. Hall, R. Kottani, G. A. N. Felton, T. Yamamoto, D. H. Evans, R. S. Glass, D. L. Lichtenberger, *J. Am. Chem. Soc.* **2014**, *136*, 4012–4018.
[16] J. Sun, M. Frasconi, Z. Liu, J. C. Barnes, Y. Wang, D. Chen, C. L. Stern, J. F. Stoddart, *Chem. Commun.* **2012**, *51*, 1432–1435.
[17] N. Hafezi, J. M. Holcroft, K. J. Hartlieb, E. J. Dale, N. A. Vermeulen, C. L. Stern, A. A. Sarjeant, J. F. Stoddart, *Angew. Chem. Int. Ed.* **2014**, *54*, 456–461.
[18] M. Kivala, C. Boudon, J.-P. Gisselbrecht, P. Seiler, M. Gross, F. Diederich, *Chem. Commun.* **2007**, 4731–4733.
[19] M. Kivala, C. Boudon, J.-P. Gisselbrecht, P. Seiler, M. Gross, F. Diederich, *Angew. Chem. Int. Ed.* **2007**, *46*, 6357–6360; *Angew. Chem.* **2007**, *119*, 6473–6477.
[20] R. S. F. Silva, E. M. Costa, Ú. L. T. Trindade, D. V. Teixeira, M. de Carmo, F. R. Pinto, G. L. Santos, V. R. S. Malta, C. Alberto De Simone, A. V. Pinto, S. L. de Castro, *Eur. J. Med. Chem.* **2006**, *41*, 526–530.
[21] G. Armendáriz-Vidales, L. S. Hernández-Muñoz, F. J. González, A. A. de Souza, F. C. de Abreu, G. A. M. Jardim, E. N. da Silva, M. O. F. Goulart, C. Frontana, *J. Org. Chem.* **2014**, *79*, 5201–5208.

[22] T. Yamagata, J. Kuwabara, T. Kanbara, *Eur. J. Org. Chem.* **2012**, 5282–5290.
[23] J. E. Kwon, C.-S. Hyun, Y. J. Ryu, J. Lee, D. J. Min, M. J. Park, B.-K. An, S. Y. Park, *J. Mater. Chem. A* **2018**, *6*, 3134–3140.
[24] J. Shukla, M. R. Ajayakumar, Y. Kumar, P. Mukhopadhyay, *Chem. Commun.* **2018**, *54*, 900–903.
[25] S. T. Schneebeli, M. Frasconi, Z. Liu, Y. Wu, D. M. Gardner, N. L. Strutt, C. Cheng, R. Carmieli, M. R. Wasielewski, J. F. Stoddart, *Angew. Chem. Int. Ed.* **2013**, *52*, 13100–13104; *Angew. Chem.* **2013**, *125*, 13338–13342.
[26] D. Chen, A.-J. Avestro, Z. Chen, J. Sun, S. Wang, M. Xiao, Z. Erno, M. M. Algaradah, M. S. Nassar, K. Amine, Y. Meng, J. Fraser Stoddart, *Adv. Mater.* **2015**, *27*, 2907–2912.
[27] A. H. Endres, M. Schaffroth, F. Paulus, H. Reiss, H. Wadepohl, F. Rominger, R. Kramer, U. H. F. Bunz, *J. Am. Chem. Soc.* **2016**, *138*, 1792–1795.
[28] a) S. Kumar, J. Shukla, K. Mandal, Y. Kumar, R. Prakash, P. Ram, P. Mukhopadhyay, *Chem. Sci.* **2019**, *10*, 6482–6493; b) Y.-W. Chuang, H.-J. Yen, G.-S. Liou, *Chem. Commun.* **2013**, *49*, 9812–9814; c) M. Iyoda, M. Hasegawa, Y. Miyake, *Chem. Rev.* **2004**, *104*, 5085–5114; d) M. Bendikov, F. Wudl, *Chem. Rev.* **2004**, *104*, 4891–4946; e) P. J. Skabara, K. Müllen, M. R. Bryce, J. A. K. Howardb, A. S. Batsanovb, *J. Mater. Chem.* **1998**, *8*, 1719–1724.
[29] M. Ueda, Y. Misaki, *Org. Lett.* **2013**, *15*, 3824–3827.
[30] D. Sakamaki, A. Ito, K. Furukawa, T. Kato, M. Shiro, K. Tanaka, *Angew. Chem. Int. Ed.* **2012**, *51*, 12776–12781; *Angew. Chem.* **2012**, *124*, 12948–12953.
[31] D. Sakamaki, A. Ito, K. Tanaka, K. Furukawa, T. Kato, M. Shiro, *Angew. Chem. Int. Ed.* **2012**, *51*, 8281–8285; *Angew. Chem.* **2012**, *124*, 8406–8410.
[32] R. Rathore, C. L. Burns, M. I. Deselnicu, *Org. Lett.* **2001**, *3*, 2887–2890.
[33] K. Katsuma, Y. Shirota, *Adv. Mater.* **1998**, *10*, 223–226.
[34] M. Hasegawa, H. Enozawa, Y. Kawabata, M. Iyoda, *J. Am. Chem. Soc.* **2007**, *129*, 3072–3073.
[35] Takase, N. Yoshida, T. Nishinaga, M. Iyoda *Org. Lett.* **2011**, *13*, 3896–3899.
[36] a) D. F. Perepichka, M. R. Bryce, I. F. Perepichka, S. B. Lyubchik, C. A. Christensen, N. Godbert, A. S. Batsanov, E. Levillain, E. J. L. McInnes, J. P. Zhao, *J. Am. Chem. Soc.* **2002**, *124*, 14227–14238; b) J. Casado-Montenegro, E. Marchante, N. Crivillers, C. Rovira, M. Mas-Torrent, *ChemPhysChem* **2016**, *17*, 1810–1814.
[37] a) A. R. Howells, A. Sankarraj, C. Shannon, *J. Am. Chem. Soc.* **2004**, *126*, 12258–12259; b) I. Kaur, W. Jia, R. P. Kopreski, S. Selvarasah, M. R. Dokmeci, C. Pramanik, N. E. McGruer, G. P. Miller, *J. Am. Chem. Soc.* **2008**, *130*, 16274–16286; c) C.-M. Chou, S. Saito, S. Yamaguchi, *Org. Lett.* **2014**, *16*, 2868–2871.
[38] P. Gautam, R. Sharma, R. Misra, M. L. Keshtov, S. A. Kuklinb, G. D. Sharma, *Chem. Sci.* **2017**, *8*, 2017–2024.
[39] K. Lincke, A. F. Frellsen, C. R. Parker, A. D. Bond, O. Hammerich, M. B. Nielsen, *Angew. Chem. Int. Ed.* **2012**, *51*, 6099–6102; *Angew. Chem.* **2012**, *124*, 6203–6206.
[40] D. F. Perepichka, M. R. Bryce, C. Pearson, M. C. Petty, E. J. L. McInnes, J. P. Zhao, *Angew. Chem. Int. Ed.* **2003**, *42*, 4636–4639; *Angew. Chem.* **2003**, *115*, 4784–4787.
[41] D. F. Perepichka, M. R. Bryce, A. S. Batsanov, E. J. L. McInnes, J. P. Zhao, R. D. Farley, *Chem. Eur. J.* **2002**, *8*, 4656–4569.
[42] C. Zhu, X. Ji, D. You, T. L. Chen, A. U. Mu, K. P. Barker, L. M. Klivansky, Y. Liu, L. Fang, *J. Am. Chem. Soc.* **2018**, *140*, 18173–18182.
[43] T. Higashino, M. S. Rodrguez-Morgade, A. Osuka, T. Torres, *Chem. Eur. J.* **2013**, *19*, 10353–10359.
[44] a) D. Asthana, M. R. Ajayakumar, R. P. Pant, P. Mukhopadhyay, *Chem. Commun.* **2012**, *48*, 6475–6477; b) S. K. Keshri, D. Asthana, S. Chorol, Y. Kumar, P. Mukhopadhyay, *Chem. Eur. J.* **2018**, *24*, 1821.
[45] J. Shukla, M. R. Ajayakumar, P. Mukhopadhyay, *Org. Lett.* **2018**, *20*, 7864–7868.
[46] Z. Li, T. Y. Gopalakrishna, Y. Han, Y. Gu, L. Yuan, W. Zeng, D. Casanova, J. Wu, *J. Am. Chem. Soc.* **2019**, *141*, 16266–16270.
[47] L. Feng, M. Rudolf, O. Trukhina, Z. Slanina, F. Uhlik, X. Lu, T. Torres, D. M. Guldi, T. Akasaka, *Chem. Commun.* **2015**, *51*, 330–333.
[48] a) S. L. Schiavo, G. Pocsfalvi, S. Serroni, P. Cardiano, P. Piraino, *Eur. J. Inorg. Chem.* **2000**, 1371–1375; b) N. R. de Tacconi, R. O. Lezna, R. Chitakunye, F. M. MacDonnell, *Inorg. Chem.* **2008**, *47*, 8847–8858.
[49] C. Dutan, S. Shah, R. C. Smith, S. Choua, T. Berclaz, M. Geoffroy, J. D. Protasiewicz, W. Kaim, B. Schwederski, Akbey. Dogan, J. Fiedler, C. J. Kuehl, P. J. Stang, *Inorg. Chem.* **2002**, *41*, 4025–4028.
[50] M. Ruben, E. Breuning, M. Barboiu, J.-P. Gisselbrecht, J.-M. Lehn, *Chem. Eur. J.* **2003**, *9*, 291–299.
[51] H. Zhylitskaya, J. Cybińska, P. Chmielewski, T. Lis, M. Stępień, *J. Am. Chem. Soc.* **2016**, *138*, 11390–11398.
[52] S. L. Schiavo, S. Serroni, F. Puntoriero, G. Tresoldi, P. Piraino, *Eur. J. Inorg. Chem.* **2002**, *286*, 79–86.
[53] C.-J. Yao, Y.-W. Zhong, J. Yao, *Inorg. Chem.* **2013**, *52*, 4040–4045.
[54] S. A. Cook, J. A. Bogart, N. Levi, A. C. Weitz, C. Moore, A. L. Rheingold, J. W. Ziller, M. P. Hendrich, A. S. Borovik, *Chem. Sci.* **2018**, *9*, 6540–654.
[55] C.-C. You, F. Würthner, *J. Am. Chem. Soc.* **2003**, *125*, 9716–9725.
[56] D. Astruc, *Nat. Chem.* **2012**, *4*, 255–267.
[57] C. Ornelas, J. Ruiz, C. Belin, D. Astruc, *J. Am. Chem. Soc.* **2009**, *131*, 590–601.
[58] T. Asatani, Y. Nakagawa, Y. Funada, S. Sawa, H. Takeda, T. Morimoto, K. Koike, O. Ishitani, *Inorg. Chem.* **2014**, *53*, 7170–7180.
[59] H. Sato, L. Miya, K. Mitsumoto, T. Matsumoto, T. Shiga, G. N. Newton, H. Oshio, *Inorg. Chem.* **2013**, *52*, 9714–9716.
[60] C. Blasco, S. Bruña, I. Cuadrado, E. Delgado, E. Hernández, *Organometallics* **2012**, *31*, 2715–2719.
[61] M. Zamora, B. Alonso, C. Pastor, I. Cuadrado, *Organometallics* **2007**, *26*, 5153–5164.
[62] a) W. Geuder, S. Hunig, A. Suchy, *Angew. Chem. Int. Ed.* **1983**, *22*, 489–490; *Angew. Chem.* **1983**, *95*, 501–502; b) B. Odell, M. V. Reddington, A. M. Z. Slawin, N. Spencer, J. Fraser Stoddart, D. J. Williams, *Angew. Chem. Int. Ed.* **1988**, *27*, 1547–1550; *Angew. Chem.* **1988**, *100*, 1605–1608; c) J. F. Stoddart, *Angew. Chem. Int. Ed.* **2017**, *56*, 11094–11125; *Angew. Chem.* **2017**, *129*, 11244–11277; d) J. C. Barnes, A. C. Fahrenbach, D. Cao, S. M. Dyar, M. Frasconi, M. A. Giesener, D. Benítez, E. Tkatchouk, O. Chernyashevskyy, W. H. Shin, H. Li, S. Sampath, C. L. Stern, A. A. Sarjeant, K. J. Hartlieb, Z. Liu, R. Carmieli, Y. Y. Botros, J. W. Choi, A. M. Z. Slawin, J. B. Ketterson, M. R. Wasielewski, W. A. Goddard III, J. F. Stoddart, *Science* **2013**, *339*, 429.
[63] J. C. Barnes, E. J. Dale, A. Prokofjevs, A. Narayanan, I. C. G. -Hall, M. Jurícek, C. L. Stern, A. A. Sarjeant, Y. Y. Botros, S. I. Stupp, J. F. Stoddart, *J. Am. Chem. Soc.* **2015**, *137*, 2392–2399.
[64] H. Wu, Y. Chen, L. Zhang, O. Anamimoghadam, D. Shen, Z. Liu, K. Cai, C. Pezzato, C. L. Stern, Y. Liu, J. F. Stoddart, *J. Am. Chem. Soc.* **2019**, *141*, 1280–1289.
[65] C. J. Bruns, M. Frasconi, J. Iehl, K. J. Hartlieb, S. T. Schneebeli, C. Cheng, S. I. Stupp, J. F. Stoddart, *J. Am. Chem. Soc.* **2014**, *136*, 4714–4723.
[66] a) T. Jiao, K. Cai, J. N. Nelson, Y. Jiao, Y. Qiu, G. Wu, J. Zhou, C. Cheng, D. Shen, Y. Feng, Z. Liu, M. R. Wasielewski, J. F. Stoddart, H. Li, *J. Am. Chem. Soc.* **2019**, *141*, 16915–16922; b) S. Kumar, M. R. Ajayakumar, G. Hundal, P. Mukhopadhyay, *J. Am. Chem. Soc.* **2014**, *136*, 12004–12010.
[67] Q. Chen, J. Sun, P. Li, I. Hod, P. Z. Moghadam, Z. S. Kean, R. Q. Snurr, J. T. Hupp, O. K. Farha, J. F. Stoddart, *J. Am. Chem. Soc.* **2016**, *138*, 14242–1424.
[68] J. S. Park, E. Karnas, K. Ohkubo, P. Chen, K. M. Kadish, S. Fukuzumi, C. W. Bielawski, T. W. Hudnall, V. M. Lynch, J. L. Sessler, *Science* **2010**, *329*, 1324–1328.
[69] a) V. Balzani, A. Credi, M. Venturi, *ChemSusChem* **2008**, *1*, 26–58; b) L. A. Malin, A. Abrahamsson, H. B. Baudin, A. Tran, C. Philouze, K. E. Berg, M. K. Raymond-Johansson, L. Sun, B. Åkermark, S. Styring, L. Hammarström, *Inorg. Chem.* **2002**, *41*, 1534–1544.
[70] a) T. J. Meyer, *Acc. Chem. Res.* **1989**, *22*, 163–170; b) M. R. Wasielewski, *Chem. Rev.* **1992**, *92*, 435–461.
[71] J. H. Alstrum-Acevedo, M. K. Brennaman, T. J. Meyer, *Inorg. Chem.* **2005**, *44*, 6802–6827.
[72] V. Artero, M. Fontecave, *Chem. Soc. Rev.* **2013**, *42*, 2338–2356.
[73] L. Hammarstrom, *Acc. Chem. Res.* **2015**, *48*, 840–850.
[74] T. Kikuchi, K. Tanaka, *Eur. J. Inorg. Chem.* **2014**, 607–618.
[75] a) M. Yagi, M. Kaneko, *Chem. Rev.* **2001**, *101*, 21–36; b) H. Lv, Y. V. Geletii, C. Zhao, J. W. Vickers, G. Zhu, Z. Luo, J. Song, T. Lian, D. G. Musaev, C. L. Hill, *Chem. Soc. Rev.* **2012**, *41*, 7572–7589.
[76] S. W. Gersten, G. J. Samuels, T. J. Meyer, *J. Am. Chem. Soc.* **1982**, *104*, 4029–4030.
[77] J. P. Collins, J. P. Sauvage, *Inorg. Chem.* **1986**, *25*, 135–141.
[78] Y. Naruta, M. Sasayama, T. Sasaki, *Angew. Chem. Int. Ed. Engl.* **1994**, *33*, 1839–1841.
[79] a) L. Duan, C. M. Araujo, M. S. G. Ahlquist, L. Sun, *Proc. Natl. Acad. Sci. USA* **2012**, *109*, 15584–15588; b) L. Duan, F. Bozoglian, S. Mandal, B. Stewart, T. Privalov, A. Llobet, L. Sun, *Nat. Chem.* **2012**, *4*, 418–423.
[80] Y. Gao, X. Ding, J. Liu, L. Wang, Z. Lu, L. Li, L. Sun, *J. Am. Chem. Soc.* **2013**, *135*, 4219–4222.
[81] M. Armand, J. M. Tarascon, *Nature* **2008**, *451*, 652–657.

[82] X.-P. Gao, H.-X. Yang, *Energy Environ. Sci.* **2010**, *3*, 174–189.
[83] Y. Morita, S. Nishida, T. Murata, M. Moriguchi, A. Ueda, M. Satoh, K. Arifuku, K. Sato, T. Takui, *Nat. Mater.* **2011**, *10*, 947–951.
[84] S. Renault, D. Brandell, T. Gustafsson, K. Edström, *Chem. Commun.* **2013**, *49*, 1945–1947.
[85] M. Yao, *J. Power Sources* **2010**, *195*, 8336–8340.
[86] W. G. Kuhr, A. R. Gallo, R. W. Manning, C. W. Rhodine, *MRS Bull.* **2004**, *29*, 838–842.
[87] K. M. Roth, N. Dontha, R. B. Dabke, D. T. Gryko, C. Clausen, J. S. Lindsey, D. F. Bocian, W. G. Kuhr, *J. Vac. Sci. Technol. B* **2000**, *18*, 2359–2364.
[88] J. S. Lindsey, D. F. Bocian, *Acc. Chem. Res.* **2011**, *44*, 638–650.
[89] a) A. J. Esswein, D. G. Nocera, *Chem. Rev.* **2007**, *107*, 4022–4047; b) V. Artero, M. Fontecave, *Coord. Chem. Rev.* **2005**, *249*, 1518–1535.
[90] S. S. Stahl, J. A. Labinger, *Angew. Chem. Int. Ed.* **1998**, *37*, 2180–2192; *Angew. Chem.* **1998**, *110*, 2298–2311.
[91] N. S. Lewis, D. G. Nocera, *Proc. Natl. Acad. Sci. USA* **2006**, *103*, 15729–15735.
[92] R. R. Schrock, *Acc. Chem. Res.* **2005**, *38*, 955–962.
[93] a) N. A. Ketterer, H. Fan, K. J. Blackmore, X. Yang, J. W. Ziller, M.-H. Baik, A. F. Heyduk, *J. Am. Chem. Soc.* **2008**, *130*, 4364–4374; b) M. R. Haneline, A. F. Heyduk, *J. Am. Chem. Soc.* **2006**, *128*, 8410–8411.
[94] R. A. Zarkesh, J. W. Ziller, A. F. Heyduk, *Angew. Chem. Int. Ed.* **2008**, *47*, 4715–4718; *Angew. Chem.* **2008**, *120*, 4793–4796.
[95] K. J. Blackmore, N. Lal, J. W. Ziller, A. F. Heyduk, *J. Am. Chem. Soc.* **2008**, *130*, 2728–2729.
[96] a) T. Horlacher, P. H. Seeberger, *Chem. Soc. Rev.* **2008**, *37*, 1414–1422; b) R. Jelinek, S. Kolusheva, *Chem. Rev.* **2004**, *104*, 5987–6015.
[97] a) M. Mehrvar, M. Abdi, *Anal. Sci.* **2004**, *20*, 1113–1126; b) B. Pejcic, B. R. D. Marco, G. Parkinson, *Analyst* **2006**, *131*, 1079–1090.
[98] D. Li, S. P. Song, C. H. Fan, *Acc. Chem. Res.* **2010**, *43*, 631–641.
[99] F. Li, Z. Yua, X. Yub, G. Zhanga, Y. Songa, H. Yana, X. Li, *Sens. Actuators B* **2015**, *220*, 1–4.
[100] M. C. Martos-Maldonado, J. M. Casas-Solvas, I. Quesada-Soriano, L. García-Fuentes, A. Vargas-Berenguel, *Langmuir* **2013**, *29*, 1318–1326.
[101] S. Kumar, Y. Kumar, S. K. Keshri, P. Mukhopadhyay, *Magnetochemistry*, **2016**, *2*, 42.

Manuscript received: November 17, 2019
Revised manuscript received: January 30, 2020